Energy losses in compound open channels

Sébastien Proust, D. Bousmar, Nicolas Riviere, André Paquier, Y. Zech

Author-produced version of the article published in Advances in Water Resources, 2010, 33 (1), 1-16
The original publication is available at http://www.sciencedirect.com/, doi:10.1016/j.advwatres.2009.10.003

Energy losses in compound open channels

S. Proust [(1)], **D. Bousmar** [(2)], **N. Rivière** [(3)], **A. Paquier** [(1)], **Y. Zech** [(4)]
[(1)] Cemagref, Hydrology-Hydraulics Research Unit, 3 bis quai Chauveau CP220, 69336 Lyon, Cedex 09, France; sebastien.proust@cemagref.fr (corresponding author)
[(2)] Hydraulic Research Laboratory, Service Public de Wallonie, Rue de l'Abattoir 164, 6200 Châtelet, Belgium; didier.bousmar@spw.wallonie.be
[(3)] Fluid Mechanics and Acoustics Laboratory (UMR CNRS 5509), INSA de Lyon, Bat Jacquard, 20 av A Einstein, 69621 Villeurbanne Cedex, France; nicolas.riviere@insa-lyon.fr
[(4)] Civil and Environmental Engineering Unit, Université catholique de Louvain, Place du Levant 1, B-1348 Louvain-la-Neuve, Belgium; yves.zech@uclouvain.be

Abstract

This paper investigates energy losses in compound channel under non-uniform flow conditions. Using the first law of thermodynamics, the concepts of energy loss and head loss are first distinguished. They are found to be different within one sub-section (main channel or floodplain). Experimental measurements of the head within the main channel and the floodplain are then analyzed for geometries with constant or variable channel width. Results show that head loss differs from one sub-section to another: the classical 1D hypothesis of unique head loss gradient appears to be erroneous. Using a model that couple 1D momentum equations, called ``Independent Sub-sections Method (ISM)", head losses are resolved. The relative weights of head losses related to bed friction, turbulent exchanges and mass transfers between sub-sections are estimated. It is shown that water level and the discharge distribution across the channel are influenced by turbulent exchanges for a) developing flows in straight channels, but only when the flow tends to uniformity; b) flows in skewed floodplains and symmetrical converging floodplains for small relative flow depth; c) flows in symmetrical diverging floodplains for small and medium relative depth. Flow parameters are influenced by the momentum flux due to mass exchanges in all non-prismatic geometries for small and medium relative depth, while this flux is negligible for developing flows in straight geometry. The role of an explicit modeling of mass conservation between sub-sections is eventually investigated.

Keywords: Compound Channel, Non-uniform flow, Energy loss, Head loss, Momentum transfer, Turbulent exchange, Mass conservation

1. Introduction

For nearly four decades, studies on compound channel flow focused on the momentum exchange between the flow in the main channel and the flow in the floodplain, in case where the overall channel width is constant. The most investigated flow configuration was uniform flow in straight geometries. In particular, the shear layer between sub-sections, the secondary currents, the boundary shear stress and the apparent shear stress at the vertical interfaces between the main channel and the floodplain were depicted. The interaction between the flow in the main channel and the flow in the floodplain is investigated e.g. by Knight and Demetriou [1]. Shiono and Knight [2] showed that three sources of energy losses coexist under uniform flow conditions: bed friction, momentum flux due to both turbulent exchange and secondary currents across the total cross-section. Three other flow configurations in non-

Author-produced version of the article published in Advances in Water Resources, 2010, 33 (1), 1-16
The original publication is available at http://www.sciencedirect.com/, doi:10.1016/j.advwatres.2009.10.003

prismatic geometry with constant overall channel width were also well investigated: flow in a compound channel with a diverging left-hand floodplain and a converging right-hand floodplain, usually called skewed flows [3,4,5], flow in meandering 2-stage channels [6] or flow in a doubly meandering compound channel [7]. These former geometries highlight the role of a previous unstudied source of energy loss: the horizontal shearing located at the bank-full level in the main channel between the upper flow and the inbank flow. The last case investigated is non-uniform flow in a straight compound channel [8,9] characterized by a strong influence of the upstream discharge distribution between sub-sections on the mass transfers along a compound channel flume. When the total width of the channel is constant and the flow is non-uniform, a common characteristic between the various experiments was identified: mass transfers between flows in the main channel and the floodplains generate low variation in flow depth along the longitudinal x-axis. The streamwise variation in flow depth was even found to be negligible for a few flow configurations.

On the contrary, when the width of the overall channel is varying, the flow depth markedly vary. This was observed for flows in symmetrically converging floodplains [10], in symmetrically diverging floodplains [9,11], in a compound channel with an abrupt contraction of the floodplain [12], or in presence of a groyne set up on a floodplain perpendicularly to the main flow direction [13]. In this case, the nature of mass transfers is clearly different, as they are produced by both streamwise changes in the total width of the channel and in water depth, and consequently become stronger than when the overall channel width remains constant.

As overbank flows with varying width are quite common in the field, this paper deals with head losses for flows with constant or variable channel width. The first aim of the paper is to identify the main physical processes responsible for head losses in both contexts. The second aim is to estimate the influence of the head losses on two hydraulic parameters of interest for engineers, the flow depth and the discharge in the floodplain, for various types of geometry. The last aim is to work out the influence of an explicit modeling of mass conservation at the interfaces between sub-sections in the longitudinal evolution of hydraulic parameters. For that purpose, we use 1D energy or momentum balances within a sub-section (main channel, left-hand or right-hand floodplain), which give a synthetic overview of the predominant physical phenomena.

First, we develop the equations of energy loss and head loss applied to one sub-section or to the total cross-section of a compound channel. An original result is obtained: head loss gradient is equal to energy slope on the total cross-section, but in the sub-sections, head loss gradient differs from the energy slope. Second, we analyze the streamwise evolution of the head in the sub-sections and in the total cross-section from various experimental data sets: developing flows in straight compound geometry, flows in symmetrical diverging or converging compound channels. In particular, we test the validity of a common 1D hypothesis: equal head loss gradients in the main channel and in the floodplain. The experimental profiles of head in the sub-sections are then compared to the numerical results of a 1D-improved model, the Independent Sub-sections Method (ISM). This model enables three sources of head loss to be accounted for: 1) the classical bed friction on the solid walls; 2) the momentum flux due to the turbulent exchanges generated by the shearing between sub-sections; 3) the momentum flux due to mass exchanges between sub-sections. Using the ISM simulations, we show the difference between computed head loss gradients and energy slopes in the sub-sections. Afterwards, we examine the relative weights of the three sources of head loss in the various geometries investigated. The influence of each source of head loss on

Author-produced version of the article published in Advances in Water Resources, 2010, 33 (1), 1-16
The original publication is available at http://www.sciencedirect.com/, doi:10.1016/j.advwatres.2009.10.003

discharge distribution and flow depth is quantified. Lastly, we examine the role of the mass conservation at the interfaces between sub-sections on the flow parameters.

2. Energy loss, head loss, and momentum

In this section, equations of energy loss, head loss and momentum are developed for one dimensional compound channel flow, relying on the work of Field et al. [14] that deals with energy and momentum in 1D open channel flow.

Let us consider a fluid system in a control volume Ω bounded by a surface A_Ω presented in Fig. 1a-b. The total energy of this fluid system is denoted *E*, and the total energy per unit mass is denoted *e* [J/kg]. We assume that the gravity force is the only volume force deriving from a potential energy, and we only consider heat transfers with the solid walls, the water surface, and with the liquid interfaces between sub-sections. Under these assumptions, the total energy *e* is the sum of macroscopic kinetic energy, potential energy of the gravity force and of the internal energy per unit mass, and the first law of thermodynamics is written [see e.g. 15]

$$\frac{\partial}{\partial t}\iiint_{\Omega}\rho e d\Omega + \iint_{A_\Omega}\rho e\left(\vec{v}.d\overrightarrow{A_\Omega}\right) = -\tilde{q} - \iint_{A_\Omega}\frac{p}{\rho}\rho\left(\vec{v}.d\overrightarrow{A_\Omega}\right) + \iint_{A_\Omega}\left(\overline{\overline{\tau}}\vec{n}\right)\left(\vec{v}.dA_\Omega\right) \qquad (1)$$

where $\vec{v}$ is the local velocity vector, $\tilde{q}$ is the calorific power exchanged with the exterior of Ω [J/s], *p* is the pressure, $\overline{\overline{\tau}}$ is the tensor of viscous and turbulent shear stresses applied to surface A_Ω, $d\overrightarrow{A_\Omega} = dA_\Omega\vec{n}$, $\vec{n}$ being the unit vector perpendicular to unit surface dA_Ω.

In absence of other volume force than the gravity force, the power of external forces applied to A_Ω is the sum of the power of pressure strengths and the power of viscous and turbulent shear stresses, the second and third terms in the right-hand side of Eq. (1), respectively. We will successively consider a balance on the total compound cross-section and a balance on one sub-section (main channel, left-hand or right-hand floodplain). In both cases, the friction with air is neglected, and we assume no slip of the fluid on the solid walls ($v_{wall} = 0$).

2.1. Total cross-section

We consider here a control volume Ω extended to the total cross-section. The flux of total energy, the power of pressure strengths and shear forces are equal to zero along the solid walls (total wetted perimeter), as velocity $v_{wall} = 0$. On the contrary, they differ from zero on the entering and exiting surfaces A_1 and A_2 presented in Fig. 1b. Developing Eq. (1) on the total cross-section under steady flow leads to (see appendix A)

$$\frac{d}{dx}\left(\alpha\frac{U^2}{2g}\right) + \frac{dz}{dx} + \frac{1}{g}\frac{d\mu}{dx} + \frac{\tilde{q}}{\rho g Q\Delta x} = 0 \qquad (2)$$

where $\alpha(x) = \iint_{A(x)} u^3 dA / \left(U^3 A\right)$ is the kinetic energy correction coefficient, *U* is the mean velocity on the total cross-section area *A*, *z* is the water level, μ is the internal energy per unit mass, *Q* the total discharge with *Q* = *AU*. It is proposed in [14] to name "energy slope"

Author-produced version of the article published in Advances in Water Resources, 2010, 33 (1), 1-16
The original publication is available at http://www.sciencedirect.com/, doi:10.1016/j.advwatres.2009.10.003

(denoted S_e) the sum of the derivative along the x direction of internal energy per unit of distance and unit of weight and of the calorific power exchanged with the exterior per unit of distance and unit of weight, which is written

$$S_e = \frac{1}{g}\frac{d\mu}{dx} + \frac{\tilde{q}}{\rho g Q \Delta x} \tag{3}$$

S_e is the gradient of energy dissipated into heat by irreversible processes. Eq. (3) is the expression of local phenomena. Recalling that total head is defined as $\mathrm{H} = z + \alpha U^2/(2g)$, the two first terms in Eq. (2) are the opposite of the longitudinal gradient of total head, denoted S_H and called below "head loss gradient". Hence, Eq. (2) is written

$$S_\mathrm{H} = -\frac{d\mathrm{H}}{dx} = -\frac{\partial}{\partial x}\left(z + \alpha\frac{U^2}{2g}\right) = S_e \tag{4}$$

According to Eq. (4), head loss gradient is equal to energy slope on the total cross-section, similarly to classical open channel flow in a single cross-section. This is the expression of the equality between mean parameters of the flow and the integrated value of local phenomena on the total cross-section.

In addition to Eq. (4), the second equation governing the flow is the classical equation of momentum conservation, the 1D-Saint-Venant equation. Under steady flow without inflow or outflow, this equation is written on the total cross-section

$$\frac{dz}{dx} + \frac{1}{gA}\frac{d}{dx}\left(\beta A U^2\right) + S_f = 0 \tag{5}$$

where $\beta(x) = \iint_{A(x)} u^2 dA / \left(U^2 A\right)$ is the momentum correction coefficient, and S_f is the friction slope on the solid walls of the overall cross-section, i.e. on the total wetted perimeter.

The link between the concepts of head loss and momentum, or between β and α, is obtained by combining Eq. (4) and Eq. (5)

$$S_H = S_f + \frac{1}{A}\frac{\partial}{\partial x}\left(\beta\frac{Q^2}{gA}\right) - \frac{\partial}{\partial x}\left(\alpha\frac{1}{2g}U^2\right) \tag{6}$$

The head loss gradient on the total cross-section is the sum of the friction slope on the total wetted perimeter and of an additional head loss due to the non-uniformity of velocity across the overall channel. This non-uniformity is significant for compound channel flow, as the value of kinetic coefficient α may exceed 2 according to French [16].

2.2. Sub-section

In the following, we consider compound channels composed of a main channel and two floodplains as shown in Fig. 1c. Subscripts "*m*", "*l*", and "*r*" are used for mean values of hydraulic parameters in the main channel, the left-hand floodplain and the right-hand floodplain, respectively. Subscript "*f*" is used for "floodplain" in general (left or/and right).

Author-produced version of the article published in Advances in Water Resources, 2010, 33 (1), 1-16
The original publication is available at http://www.sciencedirect.com/, doi:10.1016/j.advwatres.2009.10.003

Subscript "*i*" is used for a sub-section in general (*i* = *m*, *l*, *r*). Two adjacent sub-sections, i.e. parallel with regard to the longitudinal direction, are identified by subscripts "*i*" and "*j*".

The head loss gradient $S_{\mathrm{H}i}$ and the energy slope S_{ei} are respectively defined as

$$S_{\mathrm{H}i} = -\frac{d\mathrm{H}_i}{dx} = -\frac{\partial}{\partial x}\left(z_i + \alpha_i \frac{U_i^2}{2g} \right) \tag{7}$$

$$S_{ei} = \frac{1}{g}\frac{d\mu_i}{dx} + \frac{\tilde{q}_i}{\rho g Q_i \Delta x} \tag{8}$$

where μ_i, $\tilde{q}_i$, Q_i, $\mathrm{z_i}$, α_i and U_i are sub-section-averaged parameters.

When considering a balance on one sub-section, the vertical surface at the interface between two adjacent sub-sections has to be accounted for (denoted $\mathrm{A_{int}}$ in Fig. 1a-b). Eq. (1) applied to one sub-volume leads to (see appendix B)

$$S_{ei} = S_{\mathrm{H}i} \pm \frac{\tau_{ij}.U_{\mathrm{int.}}.h_{\mathrm{int.}}}{\rho g Q_i} + \frac{1}{2gQ_i}\left(q_{in}\left(U_{in}^2 - \alpha_i U_i^2 \right) + q_{out}\left(\alpha_i U_i^2 - U_{out}^2 \right) \right) \tag{9}$$

with τ_{ij} = algebraic value of the shear stress acting at the vertical interface in the *x* direction between sub-sections *i* and *j*; U_{int} = depth-averaged longitudinal velocity at the interface between sub-sections *i* and *j*, with $U_{int} = U_{in}$ or U_{out}, depending on water is entering the sub-section with a lateral discharge q_{in} or leaving the sub-section with a lateral discharge q_{out}; h_{int} = water depth at the vertical interface. Discharges q_{in} and q_{out} are considered positive and are mutually exclusive.

Eq. (9) shows that "energy slope" and "head slope gradient" are distinct within a sub-section of a compound cross-section.

The second dynamic equation within the sub-section is the equation of momentum conservation, which is written [see 17,18,19]):

$$S_{fi} = -\frac{dz_i}{dx} \pm \frac{\tau_{ij.}h_{\mathrm{int.}}}{\rho g A_i} - \frac{1}{gA_i}\frac{d}{dx}\left(\beta_i A_i U_i^2 \right) + \frac{\left(U_{in}q_{in} - U_{out}q_{out} \right)}{gA_i} \tag{10}$$

where S_{fi} is the friction slope on the solid walls (bed and lateral banks), and β_i is the Boussinesq factor averaged on the sub-section.

On the right hand side of Eq. (10), the last term is related to the momentum conveyed by the lateral inflow q_{in} or the lateral outflow q_{out} through the interface between sub-sections. The products $U_{in}.q_{in}$ and $U_{out}.q_{out}$ are the terms of momentum flux (divided by ρ) due to mass exchange.

Similarly to Eq. (6), a link between $S_{\mathrm{H}i}$ and S_{fi} can be established by combining Eq. (7) and Eq. (10):

$$S_{fi} = S_{\mathrm{H}i} \pm \frac{\tau_{ij.}h_{\mathrm{int.}}}{\rho g A_i} + \frac{d}{dx}\left(\alpha_i U_i^2/(2g) \right) - \frac{1}{gA_i}\frac{d}{dx}\left(\beta_i A_i U_i^2 \right) + \frac{\left(U_{in}q_{in} - U_{out}q_{out} \right)}{gA_i} \tag{11}$$

Author-produced version of the article published in Advances in Water Resources, 2010, 33 (1), 1-16
The original publication is available at http://www.sciencedirect.com/, doi:10.1016/j.advwatres.2009.10.003

3. Head losses

It should be recalled that, under uniform flow conditions, longitudinal gradients dz_i/dx, and dz/dx are equal to the bottom slope, denoted S_o. Thus, Eq. (4) and Eq. (7) rigorously give:

$$S_{\mathrm{H}i} = S_{\mathrm{H}j} = S_{\mathrm{H}} = S_0 \qquad (12)$$

where subscripts i and j are related to two different sub-sections.

Head loss gradients are equal in the various sub-sections and in the total cross-section, and are also equal to the bottom slope S_o. Eq. (12) also demonstrates that the head loss gradient in a sub-section is independent of the interfacial dissipation associated with shear stress τ_{ij}. This is not the case for the energy slope S_{ei} since, according to Eq. (9), "$S_{ei} = S_o \pm \tau_{ij}.U_{\mathrm{int.}}.h_{\mathrm{int.}}/(\rho g Q_i)$".

3.1. Assumptions for non-uniform flow

- **Head loss gradients**

When the flow is non-uniform, inspired by Eq. (12), the most of 1D numerical models still considers equal head loss gradients in the various sub-sections and on the total cross-section. This assumption is necessary to solve the water surface profile on the total cross-section. It is also assumed that, within a sub-section, $\alpha_i = 1$ and $\beta_i = 1$ (see next paragraph). These assumptions lead to:

$$S_{\mathrm{H}i} = -\frac{dz_i}{dx} - \frac{d}{dx}\left(\frac{U_i^2}{2g}\right) = S_{\mathrm{H}j} = -\frac{dz_j}{dx} - \frac{d}{dx}\left(\frac{U_j^2}{2g}\right) = S_{\mathrm{H}} = -\frac{dz}{dx} - \frac{d}{dx}\left(\alpha\frac{U^2}{2g}\right) \qquad (13)$$

with z = mean value of water level across the total channel, z_i = mean value of water level across the sub-section, and with total head H and the sub-section-averaged head $\mathrm{H_i}$ defined as:

$$\mathrm{H}_i = z_i + U_i^2/(2g) \qquad \text{and} \qquad \mathrm{H} = z + \alpha U^2/(2g) \qquad (14)$$

- **Correction factors of kinetic energy and momentum**

Under non-uniform flow conditions, all the 1D codes assume that, within one sub-section, $\alpha_i = \beta_i = 1$. On the contrary, they account for distinct mean velocities in the main channel and in the floodplain (i.e. $\alpha \neq \beta \neq 1$). The non-uniformity of velocity between sub-sections is thus assumed to be larger than the non-uniformity of velocity within one sub-section. Assuming $\alpha_i = \beta_i = 1$ is actually essential for 1D models as they cannot work out the lateral distribution of depth-averaged streamwise velocity U_d.

Under this assumption, combining the mass conservation in a sub-section

Author-produced version of the article published in Advances in Water Resources, 2010, 33 (1), 1-16
The original publication is available at http://www.sciencedirect.com/, doi:10.1016/j.advwatres.2009.10.003

$$\frac{dA_i U_i}{dx} = q_{in} - q_{out} \tag{15}$$

with the Eq. (11) simply gives:

$$S_{\mathrm{H}i} = S_{fi} \pm \frac{\tau_{ij} h_{\mathrm{int}}}{\rho g A_i} + \frac{q_{in}\left(U_i - U_{in}\right) + q_{out}\left(U_{out} - U_i\right)}{g A_i} = S_{fi} + S_i^t + S_i^m \tag{16}$$

The head loss gradient in one sub-section can be divided into three parts: the friction slope (S_{fi}), the head loss due to shear stress τ_{ij} related to interfacial turbulent exchanges (denoted S_i^t), and the head loss due to mass exchanges (denoted S_i^m).

3.2. Experimental measurements of head

In this section, we will investigate the streamwise evolution of the head in the sub-sections and in the total cross-section, H_i and H, defined according to Eq. (14). In particular, we want to experimentally evaluate the validity of the equation (13) for various types of geometries. We use experimental data collected in three different compound channel flumes: (i) a flume located at Université catholique de Louvain-la-neuve (UCL), Belgium, with a symmetric straight geometry (Fig. 2b), with 6m-long or 4m-long diverging floodplains (denoted Dv6 and Dv4 in Fig. 2e, respectively), and with 6m-long or 2m-long converging floodplains (Cv6 and Cv2 in Fig. 2f); (ii) a flume at Laboratoire de Mécanique des Fluides et d'Acoustique (LMFA), with an asymmetric straight geometry (Fig. 2c); and (iii) a flume at Compagnie Nationale du Rhône (CNR), France, with an asymmetric straight geometry presenting a slight curvature (Fig. 2d).

- **Non-uniform flow in straight compound channel**

The first flow configuration investigated is developing flows in a straight compound channel (Fig. 2b-d). Experimental setup and results are presented and analyzed in [8,9]. In the three flumes, the upstream floodplain discharge exceeds the floodplain discharge under uniform flow conditions. This imbalance in upstream discharge distribution creates mass transfers from the floodplain towards the main channel along the flume. The streamwise profile of floodplain discharge Q_f is presented in Fig. 3. The relative flow depth h*, defined as the ratio between the flow depth in floodplain and the flow depth in main channel (h_f / h_m), is measured at mid length of the flume. The percentage of increase in floodplain discharge at $x = 0$ compared to uniform flow conditions is denoted "dQ_f (x=0)". The streamwise evolution of sub-section head H_i is presented in Fig. 4. Analyzing this figure leads to the results listed below:

- As long as the mass transfer is significant between sub-sections, the head loss gradient in the main channel $S_{\mathrm{H}m}$ differs from the head loss gradient in the floodplain $S_{\mathrm{H}f}$. In this case, $S_{\mathrm{H}f}$ is higher than the bed slope S_o, while $S_{\mathrm{H}m}$ is lower than S_o, and Eq. (13) is not valid.

- If the flow tends to uniformity at the downstream end of the flume, the head loss gradients in the sub-sections approach the value of the bed slope S_o in accordance with Eq. (12).

Author-produced version of the article published in Advances in Water Resources, 2010, 33 (1), 1-16
The original publication is available at http://www.sciencedirect.com/, doi:10.1016/j.advwatres.2009.10.003

- Given a relative depth h^*, increasing the imbalance in floodplain discharge at station $x = 0$ accentuates the difference of evolution between floodplain head and main channel head (the difference between S_{Hm} and S_{Hf} values is larger).

- For a similar upstream imbalance in floodplain discharge, the difference of evolution between H_m and H_f rises with an increasing relative depth h^* (compare Fig. 4a and 4d, or Fig. 4c and 4f).

- Head slope gradients are more sensitive to an increase in relative depth (for a given upstream imbalance) than to an increase in upstream floodplain discharge (for a given relative depth), as shown by Fig. 4a and 4f.

- **Symmetrically diverging floodplains**

The second flow configuration investigated is flows in symmetrically diverging floodplains [9,11], presented in Fig. 2e. The streamwise profiles of flow depth in the main channel are presented in Fig. 5. The geometry "Dv6" presents a diverging semi-angle δ = 3.8°, and for "Dv4", δ = 5.7°. The relative depth h* is measured here at mid length of the diverging reach. The streamwise evolution of sub-section head H_i and total head H is presented in Fig. 6. The main results are listed below, the flow configuration being identified by "Geometry/h*/Q":

- In the majority of flow cases, considering equal head loss gradients in the sub-sections is erroneous.

- Equal head-loss gradients in the sub-sections were observed for the smallest values of total discharge Q, angle δ and relative depth h^*, i.e. for configuration Dv6/0.2/12, as shown in Fig. 6a. Besides, they are equal to the bed slope: Eq. (12) appears to be relevant in this particular case. It should be noted that for this flow configuration, the streamwise variation in main channel flow depth is the smallest of the data set investigated, as shown in Fig. 5a.

- Comparing Dv6/0.2/12 and Div4/0.2/12 (Fig. 6a and 6b) shows that when increasing angle δ from 3.8° to 5.7°, the equality $S_{Hm} = S_o$ is still valid, but slope S_{Hf} becomes lower than S_0.

- The head in the floodplain is clearly more sensitive to a change in parameters angle δ, relative depth h^* or total discharge Q than is the head in the main channel.

- The evolution of floodplain head is very sensitive to an increase in δ angle or, to a lesser extent, in total discharge Q. No clear tendency was found with an increase in relative depth h^* .

- When increasing angle δ from 3.8° to 5.7°, and consequently increasing transfers between sub-sections, head loss in the floodplain S_{Hf} may be negligible, or become negative as for Dv6/0.3/20 and Dv4/0.3/20 (Fig. 6e and 6f). This phenomenon is also observed for given angle δ and relative depth h^* when rising up the total discharge (compare Dv6/0.3/16 and Dv6/0.3/20 in Fig. 6d and 6f).

- For the highest relative depth h^* = 0.5 (Fig. 6c), both S_H and S_{Hi} are clearly smaller than the bed slope S_o. The energy dissipation is very low for this high relative depth. Besides, Eq. (13) appears to be valid: head loss gradients are equal in the sub-sections.

- In all cases, the evolution of the total head H is very close to the one of the main channel head H_m.

- **Symmetrically converging floodplains**

Author-produced version of the article published in Advances in Water Resources, 2010, 33 (1), 1-16
The original publication is available at http://www.sciencedirect.com/, doi:10.1016/j.advwatres.2009.10.003

The last configuration investigated is flow in symmetrically converging floodplains, Cv6 (δ = 3.8°) and Cv2 (δ = 11.2°), studied by Bousmar et al. [10,17], and presented in Fig. 2f. The streamwise profiles of flow depth in the main channel are presented in Fig. 7. The relative depth h^* is measured here at mid length of the converging reach. The experimental sub-section-averaged heads in these converging geometries are presented in Fig. 8. The main results are listed below:

- As expected, the head loss in the sub-sections between upstream and downstream boundaries rises up with a decreasing relative depth h^* (compare Fig. 8a and 8b) or with an increasing total discharge Q (compare 8c and 8d).
- For low and medium relative depth (h^* = 0.2 and 0.3), the head loss gradient in the main channel clearly differs from the head loss gradient in the floodplain. The streamwise variation of head is more significant in the floodplain, in accordance with the variation in width in this sub-section.
- For high relative depth (h^* = 0.5) and low discharge (Q = 12 l/s), the differences of evolution between floodplain head and main channel head are reduced. In this particular case, assuming equal head loss gradients in the sub-sections is less erroneous than in the other cases.

From the experimental observation of sub-section head H_i in both contexts with constant or variable overall channel width, we can conclude that flow configurations with equal head loss gradients in the sub-sections are infrequent. As a result, the equation (13) necessary for the 1D models that solve the Bernoulli or Saint-Venant equation on the total cross-section is erroneous in the majority of cases.

4. Modeling of sub-section head with coupled 1D equations

If the water surface profile is solved within each sub-section, there is no need to assume that the head loss gradients in the sub-sections are equal. This approach is used in the 1D-improved model, called "the Independent Sub-sections Method" (ISM). The ISM was developed by Proust et al. [9,18] to assess both the water level and the discharge distribution for non-uniform flows in compound channel. In this section, the streamwise profiles of sub-section head computed by the ISM are compared to the experimental results.

4.1. Equations of the Independent Sub-sections Method (ISM).

The Independent Sub-sections Method (ISM) solves a set of ordinary differential equations composed of three coupled 1D equations of water surface profile within each sub-section (main channel, left-hand and right-hand floodplains), and of a mass conservation on the total cross-section. The method was validated against experimental data for: developing flows in straight compound channels (Fig. 2b-d), flows in the Flood Channel Facility (FCF) with skewed floodplains (see Fig. 2a), flows in symmetrically converging and diverging floodplains (Fig. 2e-f) or in an abrupt contraction of the floodplain (Fig. 2g). The maximum relative errors in the calculation of the couple {flow depth, discharge} in the floodplain are {-8%;-19%} for the 46 flow cases investigated [9,19].

The ISM computes the water surface profile on each sub-section by solving an equation that combines Eq. (16) and the mass conservation in one sub-section Eq. (15) multiplied by "U_i / gA_i". By isolating the term that comes from the mass conservation, denoted Ma_i

Author-produced version of the article published in Advances in Water Resources, 2010, 33 (1), 1-16
The original publication is available at http://www.sciencedirect.com/, doi:10.1016/j.advwatres.2009.10.003

$$Ma_i = (q_{in} - q_{out})U_i/(gA_i) \tag{17}$$

the equation of water surface profile in each sub-section is written

$$\left(1 - \frac{U_i^2}{gh_i}\right)\frac{dh_i}{dx} = \frac{U_i^2}{gB_i}\frac{dB_i}{dx} + S_o - S_{fi} - S_i^t - S_i^m + Ma_i \tag{18}$$

with S_i^t = head loss (or gain) due to interfacial turbulent exchange, S_i^m = head loss (or gain) due to interfacial mass exchanges, and with B_i = sub-section width ($A_i = B_i.h_i$, rectangular sub-section).

The friction slope on the solid walls of the sub-section S_{fi} is computing using

$$S_{fi} = \frac{f_i}{4R_i}\frac{U_i^2}{2g} \tag{19}$$

where R_i is the hydraulic radius accounting for solid walls only, and f_i is the Darcy-Weisbach coefficient.

As previously defined in Eq. (16), the two sources of interfacial head loss S_i^t and S_i^m are respectively computed using

$$S_i^t = \pm\frac{\tau_{ij}h_{\text{int}}}{\rho g A_i} \qquad S_i^m = \frac{q_{in}(U_i - U_{in})}{gA_i} + \frac{q_{out}(U_{out} - U_i)}{gA_i} \tag{20}$$

where τ_{ij} = algebraic value of the shear stress between sub-sections *i* and *j*; and U_{in} or U_{out} = U_{int}, the depth-averaged longitudinal velocity at the interface between *i* and *j*.

In the following, we define q_{rm} (resp. q_{lm}) as the lateral mass discharge between the right-hand floodplain (resp. the left-hand floodplain) and the main channel. Both are positive if mass is leaving the floodplains, and negative if mass is entering the floodplains, i.e. in a mathematical way: $q_{out} = q_{lm}$ and $q_{in} = 0$ in the left floodplain; $q_{out} = q_{rm}$ and $q_{in} = 0$ in the right floodplain; $q_{out} = 0$ and $q_{in} = q_{lm} + q_{rm}$ in the main channel.

Using these notations, Table 1 presents the terms Ma_i, S_i^m, and S_i^t for the three sub-sections. The interfacial velocities are denoted $U_{int.l}$ or $U_{int.r}$ on the left-hand or right-hand interface, respectively, as shown in Fig. 1c. The interfacial shear stresses τ_{lm} and τ_{rm} are the absolute values of τ_{ij} on the left-hand and right-hand interfaces, respectively.

It is very important to notice that the head loss due to mass exchange S_i^m is due to the inflow (or outflow) of slower water into faster water, or vice versa. S_i^m does not exist under uniform flow conditions, as the lateral mass discharge is equal to zero in this case. As a result, S_i^m is not related to the secondary currents within uniform flows observed in [2].

It is also important to notice the difference between the terms Ma_i and S_i^m. When the velocity distribution is uniform across the channel, $U_l = U_{int.l} = U_m = U_{int.r} = U_r$, there is no momentum flux due to mass exchanges between sub-sections and consequently, no head loss due to mass exchange ($S_i^m = 0$). On the contrary, the Ma_i term is not negligible with the same uniformity of velocity across the channel. In this case, mass exchange between sub-sections occurs without transferring momentum.

Author-produced version of the article published in Advances in Water Resources, 2010, 33 (1), 1-16
The original publication is available at http://www.sciencedirect.com/, doi:10.1016/j.advwatres.2009.10.003

4.2. Turbulent exchange coefficient and interfacial velocity

The shear stresses τ_{lm} and τ_{rm} on the left-hand and right-hand interfaces are modeled using the mixing length model in the horizontal plane adopted by Bousmar and Zech [19]

$$\tau_{lm} = \rho \psi^t (U_m - U_l)^2 \qquad \tau_{rm} = \rho \psi^t (U_m - U_r)^2 \qquad (21)$$

where Ψ^t = a constant coefficient of turbulent exchange. When used in the ISM, Ψ^t was calibrated under uniform flow conditions in two small-scale compound channel flumes, the LMFA and UCL flumes, and in the Flood Channel Facility for Series A3, and was found to be equal to 0.02 [18].

The modeling of the depth-averaged streamwise velocities $U_{int.l}$ and $U_{int.r}$ relies on all the experiments presented in Fig. 2. It was found that the value of interface velocity strongly depends on the direction of mass transfer (see [18]). An overview is presented below, considering two adjacent sub-sections *i* and *j*:

- when the channel is prismatic and mass transfers occur from "i" towards "j", as for developing flows in straight geometry
$$U_{\text{int}} = U_i \qquad (22)$$
- when the channel is non-prismatic and the total width is constant, as for skewed flows
$$U_{\text{int}} = U_i \quad if \quad dB_i / dx < 0 \qquad (23)$$
$$U_{\text{int}} = U_j \quad if \quad dBi / dx > 0 \qquad (24)$$
- when the channel is non-prismatic and the total width is variable, as for diverging or converging geometries (Dv4, Dv6, Cv2, Cv6, Abrupt floodplain contraction)
$$U_{\text{int}.l} = \varphi_l U_l + (1-\varphi_l) U_m \quad and \quad U_{\text{int}.r} = \varphi_r U_r + (1-\varphi_r) U_m \qquad (25)$$

where φ_l and φ_r are weighting coefficients depending on the geometry. In Eq. (25), more weight is given to the floodplain velocity (U_l or U_r) in converging geometries, while more weight is given to the main channel velocity U_m in diverging geometries.

4.3. Comparing numerical and experimental sub-section head

The flows previously investigated in section 3.2, the flows in a compound channel with skewed floodplains [4] or with an abrupt contraction of the floodplain [12] were modeled with the Independent Sub-sections Method (ISM) in [18]. To assess the influence of the different contributions to sub-section head loss (or gain) $S_{\text{H}i} = S_{fi} + S_i^t + S_i^m$ in Eq. (16) (equivalent to Eq. (18)), three types of ISM simulations were carried out: (1) accounting for the three sources of head loss; (2) only taking into account the turbulent exchanges in the momentum flux at the interfaces; (3) ignoring the total momentum flux at the interfaces, i.e. considering bed friction as the only source of dissipation. Simulations (1), (2) and (3) are labeled in the next figures "$S_f + S^t + S^m$", "$S_f + S^t$", and "S_f", respectively.

To illustrate what can be deduced from ISM simulations, Fig. 9 presents a comparison between numerical sub-section head H_i and experimental values for two flow configurations.

Author-produced version of the article published in Advances in Water Resources, 2010, 33 (1), 1-16
The original publication is available at http://www.sciencedirect.com/, doi:10.1016/j.advwatres.2009.10.003

The two diagrams demonstrate that the head loss due to mass exchange S^m is a predominant process in the two geometries, but with notable differences.

For the diverging flow (Dv6/0.3/20), the momentum flux associated with mass exchange enables the head in the floodplain to slightly increase. The flow in the floodplain receives energy from the main channel flow thanks to the momentum flux caused by mass exchange. In this context, the S^m term in the floodplain is negative (head gain) like the head slope gradient $S_{\mathrm{H}i} = S_{fi} + S_i^t + S_i^m$. Besides, we can observe that ISM reproduces distinct head slope gradients in the two sub-sections mainly thanks to this S^m term in the floodplain. In the main channel, the effect of S^m term is negligible. Fig. 9a also shows that turbulent diffusion at the interfaces is not significant enough to increase the floodplain-averaged head. Indeed, considering turbulent diffusion only ($S_{\mathrm{H}} = S_f + S^t$), leads to positive values of S_{H} (very high head loss at the entrance) that are not in agreement with experimental data.

For the converging flow presented in Fig. 9b (Cv6/0.2/10), the role of head loss (or gain) due to mass exchange S^m is also significant, but to a lesser extent than in a channel with diverging floodplains. However, the influence of this source of dissipation is demonstrated here in both the floodplain and the main channel, with positive values in the two sub-sections (head loss).

A general view of the relative weights of the three sources of head loss will be presented in section 5 for the various geometries investigated.

4.4. Comparing head loss gradient $S_{\mathrm{H}i}$ and energy slope S_{ei}

Using ISM simulations, we computed the energy slope S_{ei} according to Eq. (9) (with α_i = 1 in the ISM). Fig. 10 presents the streamwise profile of energy slope S_{ei} and head loss gradient $S_{\mathrm{H}i}$ in the main channel and the floodplain, calculated for four flow configurations in diverging geometries. According to Eq. (9), the more the turbulent diffusion or/and the momentum flux due to mass exchange at the interfaces is significant, the more the difference between S_{ei} curve and $S_{\mathrm{H}i}$ curve is notable.

The flow Dv6/0.3/12 in Fig. 10a presents slight discrepancy between S_{ei} and $S_{\mathrm{H}i}$ in the floodplain, but no difference in the main channel. We can conclude that this flow dissipates little energy between sub-sections due to the interfacial momentum flux. When increasing the discharge from 12 L/s to 20 L/s (compare Fig. 10a and 10c), discrepancy between S_{em} and $S_{\mathrm{H}m}$ appears in the main channel, and S_{ef} strongly differs from $S_{\mathrm{H}f}$ in the floodplain. Besides, S_{ef} and $S_{\mathrm{H}f}$ have opposite signs. In a similar way, for a given total discharge Q and relative depth h^*, increasing the angle δ and the mass transfers between sub-sections lead to accentuate the difference between head loss gradient and energy slope (compare e.g. Fig. 10a and 10b).

5. Main processes responsible for head losses

In this section, we will go further in the understanding of the influence on the hydraulic parameters of bed friction, turbulent diffusion, and of momentum flux due to mass

Author-produced version of the article published in Advances in Water Resources, 2010, 33 (1), 1-16
The original publication is available at http://www.sciencedirect.com/, doi:10.1016/j.advwatres.2009.10.003

exchanges. Indeed, the relative weights of these three sources of head loss vary depending on the geometry in the horizontal plane and the relative depth *h**. Using ISM simulations of 46 non-uniform flows with either constant or variable channel width, the maximum and absolute values of S_i^m / S_{fi} ratio and S_i^t / S_{fi} ratio were calculated along each flow in the two sub-sections.

5.1. Coexistence of the three sources of head loss

Fig. 11 presents the maximum absolute values of S_i^m / S_{fi} and S_i^t / S_{fi} ratios for flows with various relative depth h^* in (a) the 2-m and 6-m converging reach (Cv2 and Cv6) and in (b) the Flood Channel Facility with skewed floodplains (see Fig. 2). For the skewed flows, three geometries are investigated: $\delta = 5.1°$, inclined banks in the main channel (side slope s = 45°); $\delta = 5.1°$, vertical banks ($s = 90°$); $\delta = 9.2°$, $s = 45°$.

According to ISM simulations, the three sources of dissipation, S^m, S^t and S_f coexist in these non-prismatic geometries. However, S^m / S_f ratios are generally larger than S^t / S_f ratios. It is also interesting to notice that the orders of magnitude of S^m / S_f and S^t / S_f ratios are comparable in the small-scale flume with converging floodplains (Cv6 and Cv2) and in the large-scale flume with skewed floodplains.

Indeed, for Cv6 and Cv2, head loss due to mass exchanges S^m is of the same order of magnitude as bed friction S_f in the main channel ($S^m \approx 0.3 \times S_f$ to $0.85 \times S_f$), while S^t can reach 66% of the S_f value in the floodplain. For flows in skewed floodplains, S^m / S_f is in the range 0.15 to 0.9 in the diverging left-hand floodplain and main channel, while S^t / S_f is less than 0.25 in the converging right hand floodplain.

5.2. Effect of angle δ in non-prismatic geometry

The effect of the δ angle between the main channel axis and the floodplain lateral banks is also highlighted in the Fig. 11. Arrows indicate the increase in angle δ. With an increasing δ angle, the relative weight of head loss due to mass exchange S^m increases while the relative weight of head loss due to turbulent exchanges S^t decreases. Head loss due to mass exchanges appears to occur at the expense of head loss associated with turbulent diffusion. In the skewed compound channel, the range of values is multiplied by 2 from $\delta = 5.1°$ to 9.2°.

5.3. Distinguishing converging floodplains and diverging floodplains

It is also interesting to analyze values of S^m / S_f and S^t / S_f ratios by distinguishing converging floodplains and diverging floodplains. Fig. 12a shows a comparison between the geometries Cv6 and Dv6 (same angle $\delta = 3.8°$), and Fig. 12b separates ratios in the diverging left-hand floodplain and in the converging right-hand floodplain of the skewed compound channel. A clear asymmetry is observed in the momentum flux between converging and

Author-produced version of the article published in Advances in Water Resources, 2010, 33 (1), 1-16
The original publication is available at http://www.sciencedirect.com/, doi:10.1016/j.advwatres.2009.10.003

diverging floodplains in the two figures. Diverging floodplains accentuate head loss due to mass exchange S^m compared to converging floodplains, while converging floodplains accentuate head loss due to turbulent exchange S^t compared to diverging floodplains.

This asymmetry is apparent in Fig. 12a, when comparing Dv6 and Cv6 (same δ angle and relative depth at mid-length h^*). These results are in accordance with the lateral profiles of experimental depth-averaged longitudinal velocity U_d presented in [10,11,18]. For both geometries Cv6 and Cv2, the derivative along the lateral direction y, dU_d/dy is small in the converging floodplain and marked in the main channel**,** while gradient dU_d/dy is very strong in diverging floodplain and small in the main channel for geometries Dv4 and Dv6.

In Fig. 12b, the same asymmetry in the momentum flux is observed for the skewed flows, in accordance with the experimental depth-averaged velocity U_d. Indeed, data exposed in [4] show that experimental gradients dU_d/dy are negligible in the converging right-hand floodplain, and strong in the diverging left-hand floodplain, leading to a velocity on the left interface $U_{int.l}$ very close to mean velocity in the main channel U_m, and to a velocity on the right interface $U_{int.r}$ equal to the mean velocity in the right floodplain U_r. Eq. (23) and (24) used in the ISM are in agreement with this experimental data.

5.4. Effect of streamwise variation in flow depth

Flows with constant total width can be compared with flows with varying overall width. Considering the diverging floodplain of Dv6 with δ = 3.8° (Fig. 12a) and the diverging left-hand floodplain of the skewed channel with δ = 5.1°, side slope s = 45° or 90° (Fig. 11b), S^m / S_f ratios were compared. In Dv6, $S^m / S_f \in$ [0.35; 1.9] in the diverging floodplain, while for skewed flows $S^m / S_f \in$ [0.14; 0.31] in the diverging left-hand floodplain. Consequently, with a slightly smaller δ angle, the diverging floodplain in Dv6 clearly produces higher values of S^m / S_f ratio than does the diverging left-hand floodplain of the skewed compound channel.

This demonstrates that, in addition to changes in the geometry, the longitudinal variation in flow depth strongly influences the head loss due to mass exchange S^m. The S^m / S_f ratios are more significant when the flow depth is variable.

5.5. Overview of the head losses in compound channel

All the previous results related to head losses are summed up in Table 2 (column 1). We give an overview of the main processes responsible for head losses depending on the relative depth h^* for the various types of geometry investigated. We recall that relative depth h^* is measured at mid-length of the flume for prismatic geometries, and at mid-length of the non-prismatic reaches for converging, diverging and skewed geometries.

6. The role of an explicit modeling of the mass conservation between sub-sections

Author-produced version of the article published in Advances in Water Resources, 2010, 33 (1), 1-16
The original publication is available at http://www.sciencedirect.com/, doi:10.1016/j.advwatres.2009.10.003

In the water profile equation of ISM, Eq. (18), the terms stemming from the mass conservation Ma_l, Ma_r and Ma_m (see Table 1) can play a major role in the evolution of quadruplet $\{z, U_l, U_m, U_r\}$, especially when the flow is far from equilibrium. In this case, the values of S^t and S^m can be of the same order of magnitude than S_f but can have a very little influence on the flow parameters, because the mass conservation terms Ma_i are predominant. To understand this phenomenon, two cases are treated in detail: developing flows in a straight compound channel and flows in symmetrically converging floodplains Cv6 and Cv2.

For developing flows in a straight geometry, the dB_i/dx terms vanish in Eq. (18). This context accentuates the role of mass conservation terms Ma_i in the flow evolution. Fig. 13 presents the longitudinal profiles in the floodplain of head loss terms (S^m, S_f, S^t) and of mass conservation terms Ma_i for two flow configurations presented in Fig. 3b. At the upstream boundary condition ($x = 0$), the floodplain discharge value Q_f exceeds the floodplain discharge under uniform flow conditions by + 119% and + 48% for the CNR flow and UCL flow, respectively.

Fig. 13b shows that the CNR flow is controlled by bed friction and mass conservation along almost the whole length of the reach concerned here. At the downstream boundary, flow is still far from equilibrium and consequently the value of *Ma* term differs from zero. On the contrary, as shown in Fig. 13a, the UCL flow tends to uniformity at mid-length of the reach concerned. The reach can be divided into three parts: an upstream part where the flow is mainly controlled by bed friction and mass conservation between sub-sections; a downstream part dominated by bed friction and turbulent diffusion at the interface with $|S^t/S_f \approx 0.15|$ in the floodplain; and a region of transition between the two. Consequently, as long as the flow is far from equilibrium in a straight compound channel, the mass conservation has more influence on the evolution of the discharge distribution and water level than does the interfacial momentum flux due to turbulence.

It is also interesting to compare the relative weights of mass conservation and head losses at the interfaces in converging geometries Cv6 and Cv2. Maximum absolute values of S^t / Ma and S^m / Ma ratios are shown in Fig. 14 for the 12 flows investigated. The S^t / S_f and S^m / S_f ratios were shown in Fig. 11a. Comparing the two figures, it is clear that the mass conservation terms reduce the effect of head losses at the interfaces. Indeed, the range of S^m / S_f ratios is twice as extended as the range of S^m / Ma ratios, as the S^t / Ma ratios are twice lower than the S^t / S_f ratios. For instance, the weight of S^t is negligible relative to the *Ma* term (one order of magnitude lower), except for one shallow flow, while S^t and S_f values are of the same magnitude order for four shallow flows.

As a result, we can conclude that for numerous flows, the head loss at the interfaces is not negligible but does not influence the hydraulic parameters. In this case, the quadruplet $\{z, U_l, U_m, U_r\}$ is controlled to a large extent by bed frictions and by the mass conservation between sub-sections. The interest of accurately modeling the mass conservation with an explicit law (Eq. (15)) is thus highlighted.

Related to mass exchanges at the interfaces, two distinct processes were distinguished: the mass conservation symbolized by Ma_i terms in Eq. (18); and the head loss (or gain) due to mass exchanges S^m. The relative weights of these two processes on hydraulic parameters are summed up in Table 2, column 2.

Author-produced version of the article published in Advances in Water Resources, 2010, 33 (1), 1-16
The original publication is available at http://www.sciencedirect.com/, doi:10.1016/j.advwatres.2009.10.003

7. Discussion

The comparison between experimental data and the numerical results of the ISM leads to the results listed below:

- The two predominant physical phenomena that influence the water level and the sub-section-averaged velocities $\{z, U_l, U_m, U_r\}$ are the bed friction and the mass conservation between sub-sections.
- Mass transfers have far more influence than turbulent diffusion on the interfacial head losses in all the non-prismatic geometries investigated. The contrary is observed for non-uniform flows in straight geometries.
- The flow parameters are influenced by head loss due to mass exchange (S^m) for: a) flows in diverging geometries for relative depth $h^* \leq 0.4$; b) flows in converging geometries for $h^* \leq 0.3$, and c) flows in an abrupt floodplain contraction or in skewed compound channel for $h^* \leq 0.25$.
- In symmetrical diverging geometries, S^m plays a specific role. This is a gain of head in the floodplains and this enables the floodplain head to remain constant or to increase for some flow cases.
- The flow parameters are influenced by head loss due to turbulent diffusion (S^t) for: a) developing flows in straight channel approaching the equilibrium, for relative depth $h^* \leq 0.27$; b) flows in diverging geometries for $h^* \leq 0.4$; c) flows in converging geometries or in skewed compound channel for $h^* \leq 0.25$.
- For a fixed angle δ between the floodplain lateral walls and the axis of the main channel, converging floodplains accentuate the values of S^t compared to diverging floodplains, while diverging floodplains accentuate the values of S^m compared to converging floodplains.
- With an increasing δ angle, the relative weight of head loss due to mass exchange S^m increases while the relative weight of head loss due to turbulent exchange S^t decreases.
- For a fixed angle δ, the head loss due to mass exchange S^m is higher when the flow depth is variable than when the flow depth is constant.
- For numerous flow configurations, the head losses due to mass or turbulent exchange are not negligible compared to bed friction, but their effect on the quadruplet $\{z, U_l, U_m, U_r\}$ is not sensitive, because of the predominance of mass conservation terms.

8. Conclusions

Using the first law of thermodynamics applied to a compound channel flow leads to an original result: head loss gradient is equal to energy slope on the total cross-section, but head loss gradient differs from energy slope in the main channel or the floodplain.

By examining the experimental head in the sub-sections for developing flows in straight compound channel, or flows in diverging or converging geometries, we tested the

Author-produced version of the article published in Advances in Water Resources, 2010, 33 (1), 1-16
The original publication is available at http://www.sciencedirect.com/, doi:10.1016/j.advwatres.2009.10.003

validity of a common 1D hypothesis: equal head loss in the main channel and the floodplain. In the vast majority of cases, the head loss gradient differs from one sub-section to another, in both contexts of constant or variable channel width. However, in the case of flow in diverging or converging floodplains with high relative depth ($h^* = 0.5$), the energy dissipation is low, and assuming equal head loss gradients in the sub-sections is less erroneous than in the other cases. The evolution of experimental sub-section head is very sensitive to relative depth h^* and to the angle δ between the axis of the main channel and the floodplain lateral walls; this evolution is also sensitive, to a lesser extent, to the upstream discharge distribution.

Head losses are then resolved with the help of the ISM, a 1D model that solves the water surface profile in each sub-section (main channel, left-hand and right-hand floodplains). Comparing the numerical results with the experimental data shows that the head loss due to mass exchange betweens subsections is notable in non-prismatic geometries, but is negligible in straight geometries. The head loss due to turbulent exchange is found to be important in both prismatic and non-prismatic geometries, for small and medium overbank flows. Results also demonstrate that the bed friction and the terms of mass conservation between sub-sections strongly influences the water level and the sub-section-averaged velocities $\{z, U_l, U_m, U_r\}$.

These results imply that traditional 1D approaches could fail or should be used cautiously in solving engineering problems when rivers present longitudinal changes in the geometry (with angles as low as 3.8°) or/and in the total wetted area. Indeed, classical 1D codes do not explicitly model the mass exchange between sub-sections, which is required in this context to obtain accurate results on both water depth and discharge distribution.

For field cases such as floods in valleys with variable width, the calibration of the coefficients representing the head losses in classical 1D (manning roughness, coefficients of contraction and expansion) is expected to be tricky, notably for small and medium overbank flows ($h^* \leq 0.3$). Erroneous results on both water depth and flow distribution are also expected. The more erroneous results are expected when using a 1D code that does not explicitly model the mass conservation between sub-sections, and that does not consider both turbulent exchange and momentum flux due to mass exchanges at the interface.

ACKNOWLEDGMENTS

.

Experiments in CNR flume, UCL flume, and LMFA flume were funded by research programmes PNRH 99-04 and ECCO-PNRH 05CV123. D. Bousmar, N.Rivière, and S. Proust travel costs were supported by the Tournesol programme grant 02947VM, funded by EGIDE, France, and CGRI, Communauté française de Belgique.

APPENDIX

The total energy e per unit mass is the sum of macroscopic kinetic energy, potential energy of the gravity force and of the internal energy per unit mass. Energy e is defined at point M as [15]

$$e(M) = 1/2.\left(u(M)^2 + v(M)^2 + w(M)^2\right) + gz(M) + \mu \qquad \text{(A1)}$$

where $\{u,v,w\}$are the velocity components within the orthogonal frame $\{x,y,z\}$; μ, is the internal energy per mass unit [J/kg]; z, the level of point M with respect to a reference datum.

Author-produced version of the article published in Advances in Water Resources, 2010, 33 (1), 1-16
The original publication is available at http://www.sciencedirect.com/, doi:10.1016/j.advwatres.2009.10.003

Considering one dimensional flow with mass exchange between sub-sections, we assume in the following that $w << v < u$ and that $v^2 << u^2$.

A. Equation on the total cross-section

Under steady flow, Eq. (1) becomes on the total cross-section area

$$\iint_{A_\Omega = A_1 \cup A_2} \rho e\left(\vec{v}.d\overrightarrow{A_\Omega}\right) = -\tilde{q} - \iint_{A_\Omega = A_1 \cup A_2} \frac{p}{\rho}\rho\left(\vec{v}.d\overrightarrow{A_\Omega}\right) + \iint_{A_\Omega = A_1 \cup A_2} \left(\overline{\overline{\tau}}\vec{n}\right).(\vec{v}.dA_\Omega) \quad \text{(A2)}$$

Assuming that the vertical distribution of pressure is hydrostatic, with $p(M) = \rho\, g(h - \eta(M))$ (h being the flow depth above the bottom, and $\eta(M)$, the elevation of point M above the bottom), the total energy per unit of mass e is written

$$e(M) = 1/2.\left(u(M)^2\right) + g\left(z(M)\right) + \mu \quad \text{(A3)}$$

If the shear tress τ_{xx} is assumed to be negligible compared to pressure p, Eq. (A2) is written

$$\iint_{A_\Omega = A_1 \cup A_2} \rho\left(\frac{u^2}{2} + gz + \mu\right)\left(\vec{v}.d\overrightarrow{A_\Omega}\right) + \iint_{A_\Omega = A_1 \cup A_2} \rho g(h - \eta)\left(\vec{v}.d\overrightarrow{A_\Omega}\right) + \tilde{q} \quad \text{(A4)}$$

The development of Eq. (A4) gives

$$\rho\frac{d}{dx}\left(\alpha\frac{AU^3}{2}\right)dx + \rho g\frac{d}{dx}\left(z_{bed}Q\right)dx + \rho g\frac{d}{dx}\left(hQ\right)dx + \rho\frac{d}{dx}\left(\mu Q\right)dx + \tilde{q} \quad \text{(A5)}$$

where α is the Coriolis coefficient on the total cross-section, and $z(M) = z_{bed} + \eta(M)$

Under steady flow, the total discharge $Q = AU$ is constant on the total cross-section, and Eq. (A5) is written

$$\rho Q\frac{d}{dx}\left(\alpha\frac{U^2}{2}\right)dx + \rho gQ\left(\frac{dh}{dx} - So\right)dx + \rho Q\frac{d\mu}{dx}dx + \tilde{q} = 0 \quad \text{(A6)}$$

with $S_o = -dz_{bed}/dx$

By dividing Eq. (A6) by $\rho gQdx$, it leads to Eq. (2).

B. Equation on a sub-section

Under steady flow conditions, Eq. (1) is written on the sub-section:

Author-produced version of the article published in Advances in Water Resources, 2010, 33 (1), 1-16
The original publication is available at http://www.sciencedirect.com/, doi:10.1016/j.advwatres.2009.10.003

$$\iint_{A_\Omega = A_1 \cup A_2 \cup A_{\text{int.}}} \rho e\left(\vec{v}.d\overrightarrow{A_\Omega}\right) = -\tilde{q} - \iint_{A_\Omega = A_1 \cup A_2 \cup A_{\text{int.}}} \frac{p}{\rho}\rho\left(\vec{v}.d\overrightarrow{A_\Omega}\right) + \iint_{A_\Omega = A_1 \cup A_2 \cup A_{\text{int.}}} \left(\overline{\overline{\tau}}\vec{n}\right)(\vec{v}. \quad \text{(B1)}$$

which develops in:

$$\rho\frac{d}{dx}\left(\alpha_i \frac{A_i U_i^{\,3}}{2}\right)dx + \rho g\frac{d}{dx}(z_{bed}Q_i)dx + \rho g\frac{d}{dx}(h_i Q_i)dx + \rho\frac{d}{dx}(\mu Q_i)dx + \tilde{q}...$$
$$...-\rho g q dx(z_{bed}+h) - \rho q_{in}dx.\frac{U_{in}^2}{2} + \rho q_{out}dx.\frac{U_{out}^2}{2} - \rho q\mu dx \pm \tau_{ij}U_{\text{int.}}h_{\text{int.}}d \quad \text{(B2)}$$

where subscript "*i*" is related to a sub-section *i*, $q = q_{in} - q_{out} = dQ_i/dx$, and where it is also assumed that $\tau_{xx} << p$ in the sub-section.

Eq. (B2) develops in

$$\rho Q_i\frac{d}{dx}\left(\alpha_i\frac{U_i^{\,2}}{2}\right)dx + \rho\alpha_i\frac{U_i^{\,2}}{2}(q_{in}-q_{out})dx + \rho g Q_i\left(\frac{dh_i}{dx} - So\right)dx + \rho Q_i\frac{d\mu}{dx}dx + \tilde{q}...$$
$$-\rho q_{in}dx.\frac{U_{in}^2}{2} + \rho q_{out}dx.\frac{U_{out}^2}{2} \pm \tau_{ij}.U_{\text{int.}}h_{\text{int.}}dx = 0 \quad \text{(B3)}$$

Introducing the head loss gradient S_{Hi} and the energy slope S_{ei} in one sub-section (Eq. (7) and (8)), and dividing Eq. (B3) by «$\rho g Q_i dx$ » leads to Eq. (9).

NOTATIONS

A_i = sub-section area;
B_i = sub-section width;
h_i = sub-section flow depth;
h^* = relative flow depth at mid-length of a prismatic channel or at mid-length of a diverging , converging or skewed reach;
H_i = sub-section head;
q_{in} = lateral inflow per unit length;
q_{out} = lateral outflow per unit length;
q_{rm} = lateral mass discharge between the right-hand floodplain and the main channel (algebraic value);
q_{lm} = lateral mass discharge between the left-hand floodplain and the main channel (algebraic value);
Q = total discharge;
S_0 = bed slope;
S_{fi} = sub-section friction slope;

Author-produced version of the article published in Advances in Water Resources, 2010, 33 (1), 1-16
The original publication is available at http://www.sciencedirect.com/, doi:10.1016/j.advwatres.2009.10.003

S_{Hi} = sub-section head loss gradient;
U_d = depth-averaged velocity in the longitudinal direction
U_i = sub-section mean velocity;
U_{in} = longitudinal velocity of lateral inflow q_{in} at the interface
U_{int} = longitudinal velocity at the interface between one floodplain and the main channel;
$U_{int.l}$ = longitudinal velocity at the interface between the left-hand floodplain and the main channel;
$U_{int.r}$ = longitudinal velocity at the interface between the right-hand floodplain and the main channel;
U_{out} = longitudinal velocity of lateral outflow q_{out} at the interface
x = longitudinal direction;
y = lateral direction;
z = water level above reference datum;
α = Coriolis coefficient on the total cross-section;
α_i = Coriolis coefficient in sub-section i;
β = Boussinesq coefficient on the total cross-section.
βi = Boussinesq coefficient in sub-section i;
δ = angle between the floodplain lateral walls and the main channel axis (x-direction);
τ_{ij} = shear stress at the vertical interface between two adjacent sub-sections i and j along x-axis (depth-averaged value);
ψ^t = coefficient of turbulent exchange;

Subscripts

f = concerning floodplain
i = concerning a sub-section ($i = l$, r or m)
l = concerning left-hand floodplain
m = concerning main channel
r = concerning right-hand floodplain

Author-produced version of the article published in Advances in Water Resources, 2010, 33 (1), 1-16
The original publication is available at http://www.sciencedirect.com/, doi:10.1016/j.advwatres.2009.10.003

REFERENCES

[1] Knight, D. W., and Demetriou, J. D. (1983). "Floodplain and main channel flow interaction." Journal of Hydraulic Engineering, ASCE, 109(8), 1073-1092.
[2] Shiono, K. and D. W. Knight (1991). "Turbulent open channel flows with variable depth across the channel." Journal of Fluid Mechanics 222: 617-646.
[3] Elliot, S. C. A. and R. H. J. Sellin (1990). "SERC Flood channel facility : skewed flow experiments." Journal of Hydraulic Research 28(2): 197-214.
[4] Sellin, R. H. J. (1993). SERC Flood Channel Facility : experimental data - Phase A - Skewed Floodplain Boundaries, Department of Civil Engineering, University of Bristol.
[5] Chlebek, J. and D. W. Knight (2008). Observations on flow in channels with skewed floodplains. Proc. of the 4th International Conference on Fluvial Hydraulics, River Flow 2008, Cesme-Izmir, Turkey, September 3-5, Altinakar, Kokpinar, Aydin, Cokgor & Kirkgoz (eds), 1, 519-527.
[6] Shiono, K. and Y. Muto (1998). "Complex flow mechanisms in compound meandering channels with overbank flow." Journal of Fluid Mechanics 376: 221-226.
[7] Islam, G. M. T., Y. Kawahara, Tamaï, N. (2008). Unsteady flow pattern in a doubly meandering compound channel. Proc. of the 4th International Conference on Fluvial Hydraulics, River Flow 2008, Cesme-Izmir, Turkey, September 3-5, Altinakar, Kokpinar, Aydin, Cokgor & Kirkgoz (eds), 1, 499-507.
[8] Bousmar, D., Rivière, N., Proust, S., Paquier, A., Morel, R., and Zech, Y. (2005). "Upstream discharge distribution in compound-channel flumes." Journal of Hydraulic Engineering, ASCE, 131(5), 408-412.
[9] Proust, S. (2005). "Ecoulements non-uniformes en lits composés : effets de variations de largeur du lit majeur / Non-uniform flow in compound channel: effect of variation in channel width" PhD-Thesis, INSA Lyon, n°2005-ISAL-0083, 362 p, Lyon, France, http://cemadoc.cemagref.fr/cemoa/PUB00018439.
[10] Bousmar, D., Wilkin, N., Jacquemart, J. H., and Zech, Y. (2004). "Overbank flow in symmetrically narrowing floodplains." Journal of Hydraulic Engineering, 130(4), 305-312.
[11] Bousmar, D., Proust, S., and Zech, Y. (2006) "Experiments on the flow in a enlarging compound channel." Proc. of the int. conf. on fluvial hydraulics, River flow 2006, 6-8 September, Lisbon, Portugal, 323-332.
[12] Proust, S., Rivière, N., Bousmar, D., Paquier, A., Zech, Y., and Morel, R. (2006). "Flow in compound channel with abrupt floodplain contraction." Journal of Hydraulic Engineering, American Society of Civil Engineers, 132(9), 958-970.
[13] Peltier, Y., Proust, S., Bourdat, A., Thollet, F., Rivière, N., Paquier, A. (2008). Physical and numerical modeling of overbank flows with a groyne on the floodplain. Proc. of the International Conference on Fluvial Hydraulics, River Flow, Cesme-Izmir, Turkey, September 3-5, 2008, Altinakar, Kokpinar, Aydin, Cokgor & Kirkgoz (eds), 1, 447-456.
[14] Field, W. G., Lambert, M. F., Williams, B.J. (1998). "Energy and momentum in one dimensional open channel flow." Journal of Hydraulic Research 36: 29-42.
[15] Perez, J. P. and A. M. Romulus (1993). “Thermodynamique, fondements et applications”, Masson, Paris, 564 p.
[16] French, R. H. (1985). Open Channel Hydraulics. New -York, McGraw-Hill.
[17] Bousmar, D. (2002). Flow modelling in compound channels / Momentum transfer between main channel and prismatic or non-prismatic floodplains. Ph-D thesis, Unité de Génie Civil et Environnemental, Université catholique de Louvain, Faculté des Sciences Appliquées: 306 p.
[18] Proust, S., Bousmar, D., Rivière, N., Paquier, A., and Zech, Y. (2009). "Non-uniform

flow in compound channel: a 1D-method for assessing water level and discharge distribution.", *Water Resources Research*, in press, doi:10.1029/2009WR008202
[19] Bousmar, D., Zech, Y. (1999). “Momentum transfer for practical flow computation in compound channels.” Journal of Hydraulic Engineering, 125(7), 696-706.

Author-produced version of the article published in Advances in Water Resources, 2010, 33 (1), 1-16
The original publication is available at http://www.sciencedirect.com/, doi:10.1016/j.advwatres.2009.10.003

Table 1

Terms of mass conservation and head loss within each sub-section in Eq. (18)

Terms of	Left-hand floodplain	Main channel	Right-hand floodplain
Mass conservation term Ma_i	$\frac{q_{lm}U_l}{gA_l}$	$-\frac{q_{lm}U_m}{gA_m}-\frac{q_{rm}U_m}{gA_m}$	$\frac{q_{rm}U_r}{gA_r}$
Head loss due to mass exchange S_i^m	$\frac{q_{lm}(U_{\text{int}.l}-U_l)}{gA_l}$	$\frac{q_{lm}(U_m-U_{\text{int}.l})}{gA_m}+\frac{q_{rm}(U_m-U_{\text{int}.r})}{gA_m}$	$\frac{q_{rm}(U_{\text{int}.r}-U_r)}{gA_r}$
Head loss due to turbulent exchange S_i^t	$-\frac{\tau_{lm}h_l}{\rho gA_l}$	$\frac{\tau_{lm}h_l}{\rho gA_m}+\frac{\tau_{rm}h_r}{\rho gA_m}$	$-\frac{\tau_{rm}h_r}{\rho gA_r}$

Author-produced version of the article published in Advances in Water Resources, 2010, 33 (1), 1-16
The original publication is available at http://www.sciencedirect.com/, doi:10.1016/j.advwatres.2009.10.003

Table 2

Overbank flows: 1) Main physical phenomena responsible for head losses; (2) Relative weights of terms of mass conservation and of head loss due to mass exchanges at the interfaces in Eq. (18)

Types of overbank flows	**1) Head losses: main processes**	**2) Mass exchange: Relative weights of Ma_i term and S_i^m term in Eq. (18)**
Uniform flow	- Bed friction - Interfacial turbulent exchange - Momentum flux due to secondary currents	Nil
Non-uniform flow in straight geometry:		
a) far from equilibrium	a) Bed friction	a) Conservation >> momentum flux
b) slightly destabilized	b) Bed friction and interfacial turbulent exchange for $h^* \leq 0.27$.	b) Conservation > momentum flux
Skewed floodplains (5.1°, 9.2°)	- Bed friction - Interfacial turbulent exchange for $h^* \leq 0.25$ - Momentum due to mass exchange in the diverging left floodplain only, for $h^* \leq 0.25$.	Conservation > momentum flux
Symmetrically converging floodplains (3.8°, 11.2°)	- Bed friction - Interfacial turbulent exchange for $h^* \leq 0.2$. - Momentum transfer due to mass exchange for $h^* \leq 0.3$.	Conservation > momentum flux
Abrupt contraction of the floodplain (22°)	- Bed friction - Momentum transfer due to mass exchange for $h^* \leq 0.23$. .	Conservation > momentum flux
Symmetrically diverging floodplains (3.8°, 5.7°)	- Bed friction - Interfacial turbulent exchange for $h^* \leq 0.4$) - Strong momentum transfer due to mass exchange for $h^* \leq 0.4$.	Conservation ≈ momentum flux (for 2 flow cases) Conservation > momentum flux (for 10 flow cases)

Nb: relative depth h^* is measured at mid-length of the prismatic or non-prismatic reach.

Author-produced version of the article published in Advances in Water Resources, 2010, 33 (1), 1-16
The original publication is available at http://www.sciencedirect.com/, doi:10.1016/j.advwatres.2009.10.003

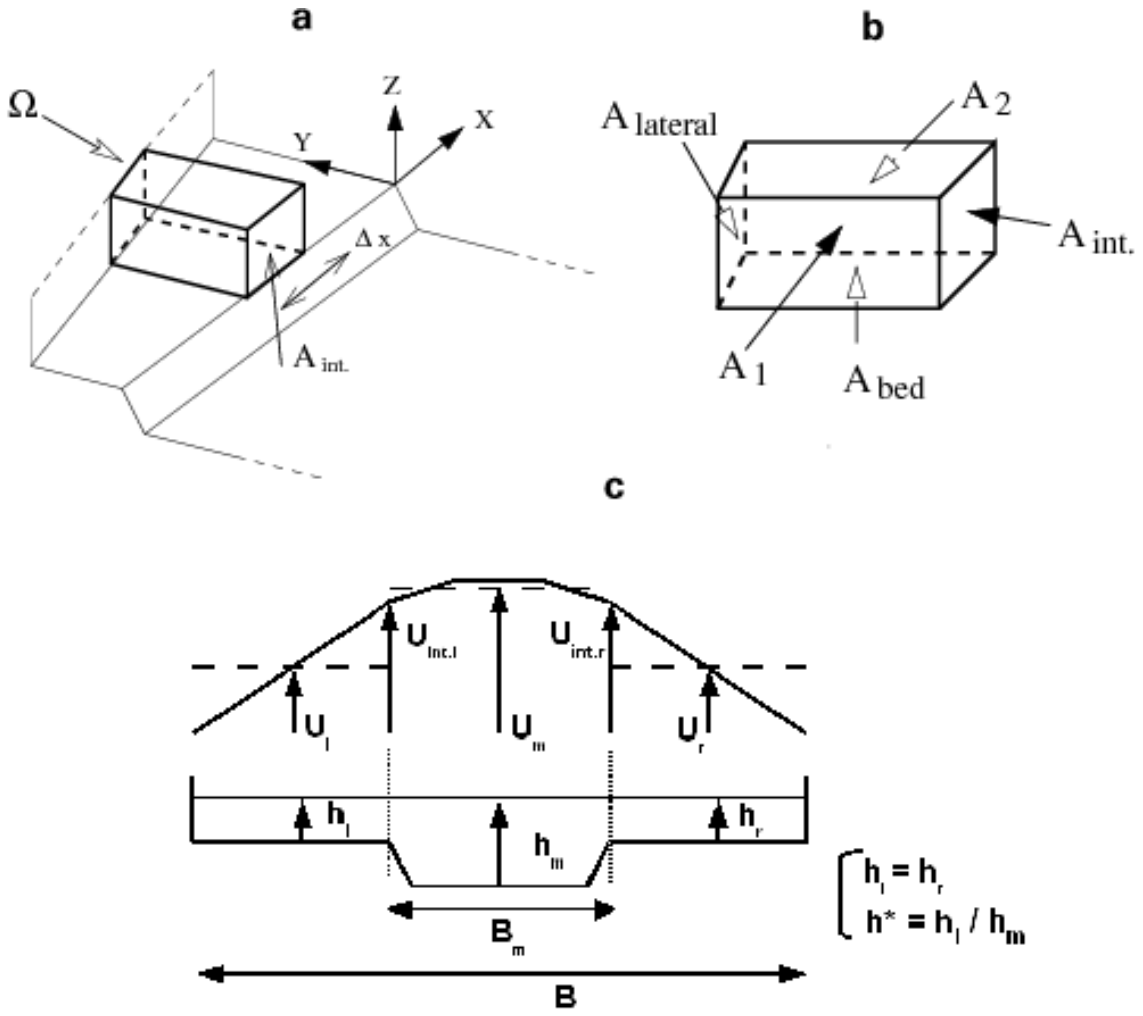

Fig. 1. Schematic view of a fluid system in a control volume Ω, bounded by a surface A_Ω (a,b) with $A_\Omega = A_{lateral} \cup A_{bed} \cup A_{\text{int}} \cup A_1 \cup A_2$; c) notations of hydraulic and geometrical parameters

Author-produced version of the article published in Advances in Water Resources, 2010, 33 (1), 1-16
The original publication is available at http://www.sciencedirect.com/, doi:10.1016/j.advwatres.2009.10.003

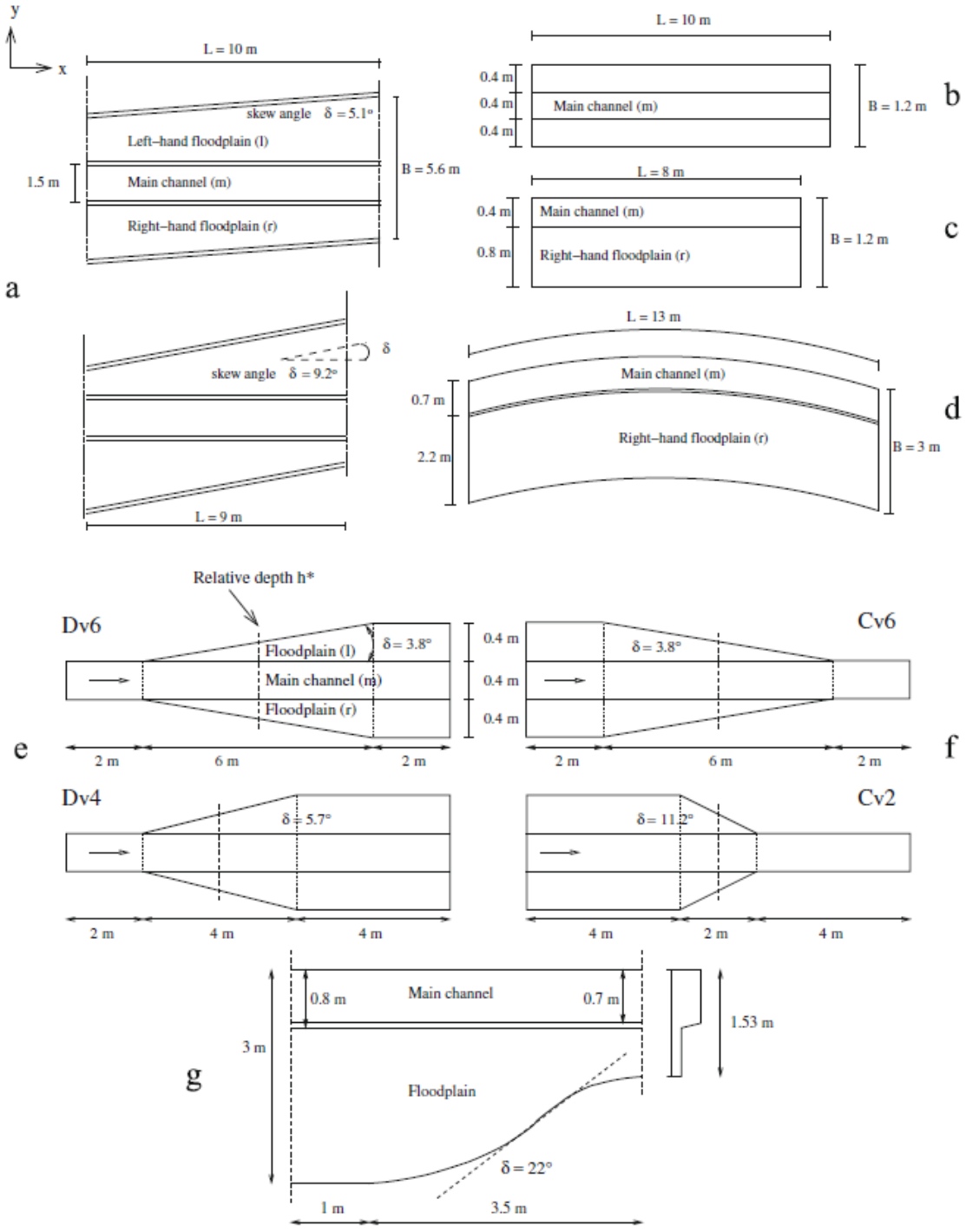

Fig. 2. Top view of the compound channels with skewed floodplains (a), straight geometries (b-d), diverging geometries Dv6 and Dv4 (e), converging geometries Cv6 and Cv2 (f), abrupt floodplain contraction (g).

Author-produced version of the article published in Advances in Water Resources, 2010, 33 (1), 1-16
The original publication is available at http://www.sciencedirect.com/, doi:10.1016/j.advwatres.2009.10.003

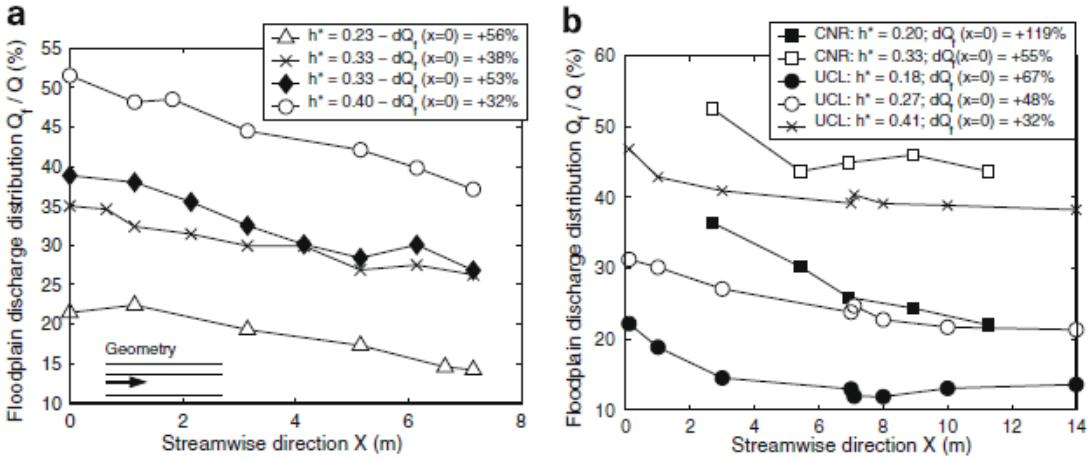

Fig. 3. Developing flows in straight compound channels: experimental measurements of floodplain discharge distribution Q_f / Q (%) in (a) LMFA flume and in (b) CNR and UCL flumes.

Author-produced version of the article published in Advances in Water Resources, 2010, 33 (1), 1-16
The original publication is available at http://www.sciencedirect.com/, doi:10.1016/j.advwatres.2009.10.003

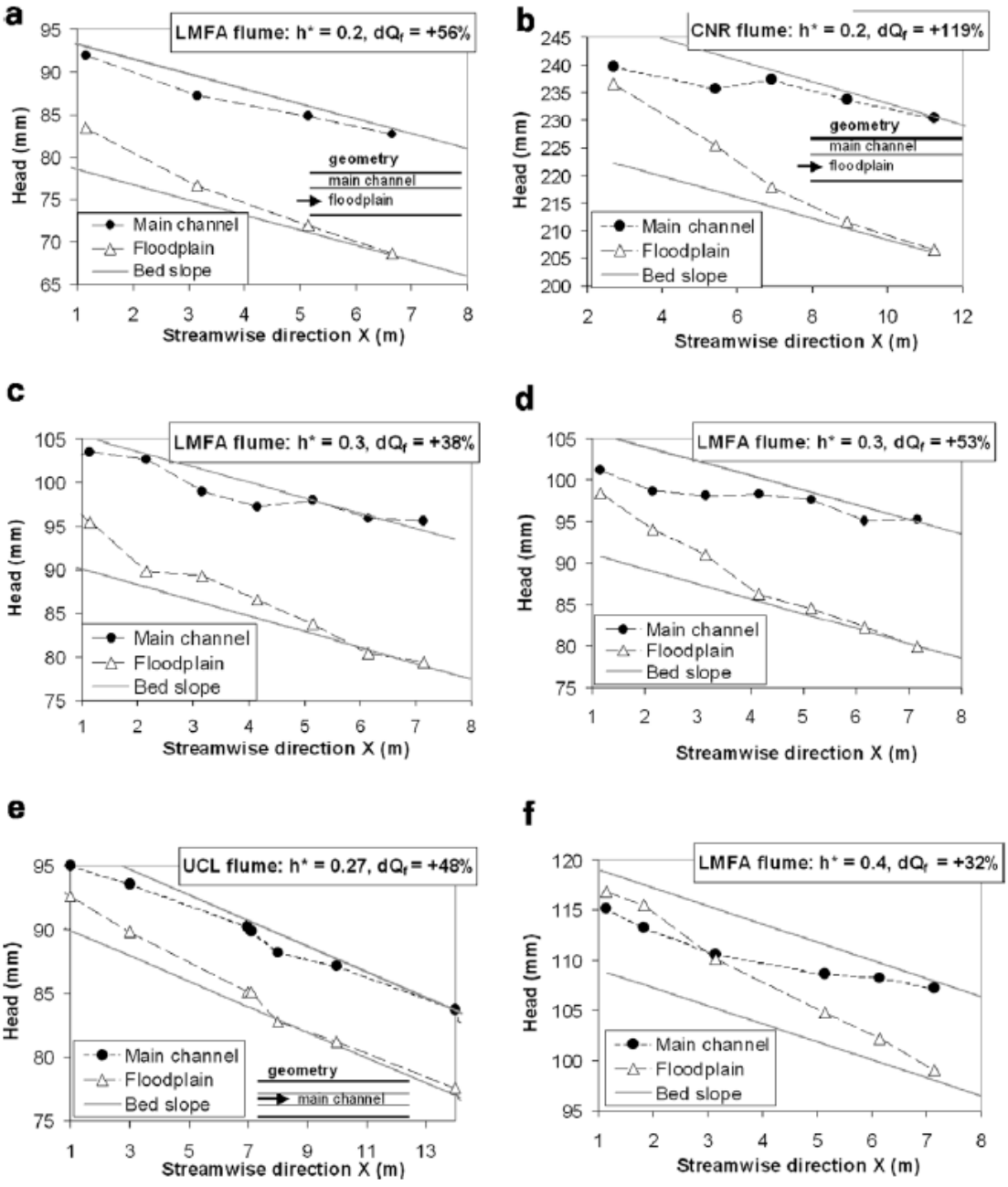

Fig. 4. Developing flows in straight compound channel: experimental measurements of sub-section-averaged head H_i

Author-produced version of the article published in Advances in Water Resources, 2010, 33 (1), 1-16
The original publication is available at http://www.sciencedirect.com/, doi:10.1016/j.advwatres.2009.10.003

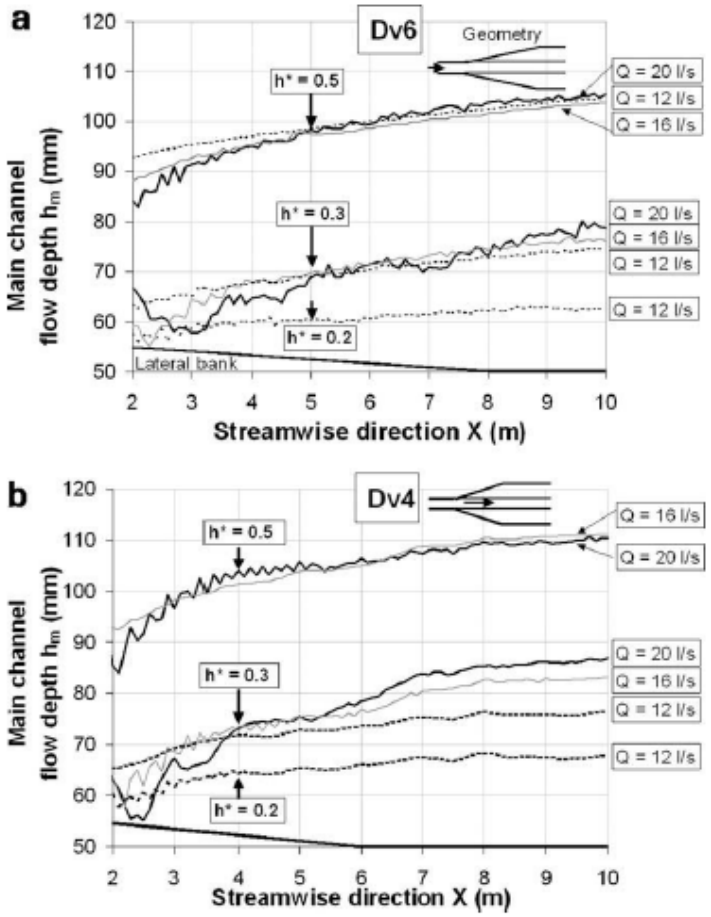

Fig. 5. Longitudinal profile of experimental flow depth in the main channel for diverging geometries Dv6 (a) and Dv4 (b).

Author-produced version of the article published in Advances in Water Resources, 2010, 33 (1), 1-16
The original publication is available at http://www.sciencedirect.com/, doi:10.1016/j.advwatres.2009.10.003

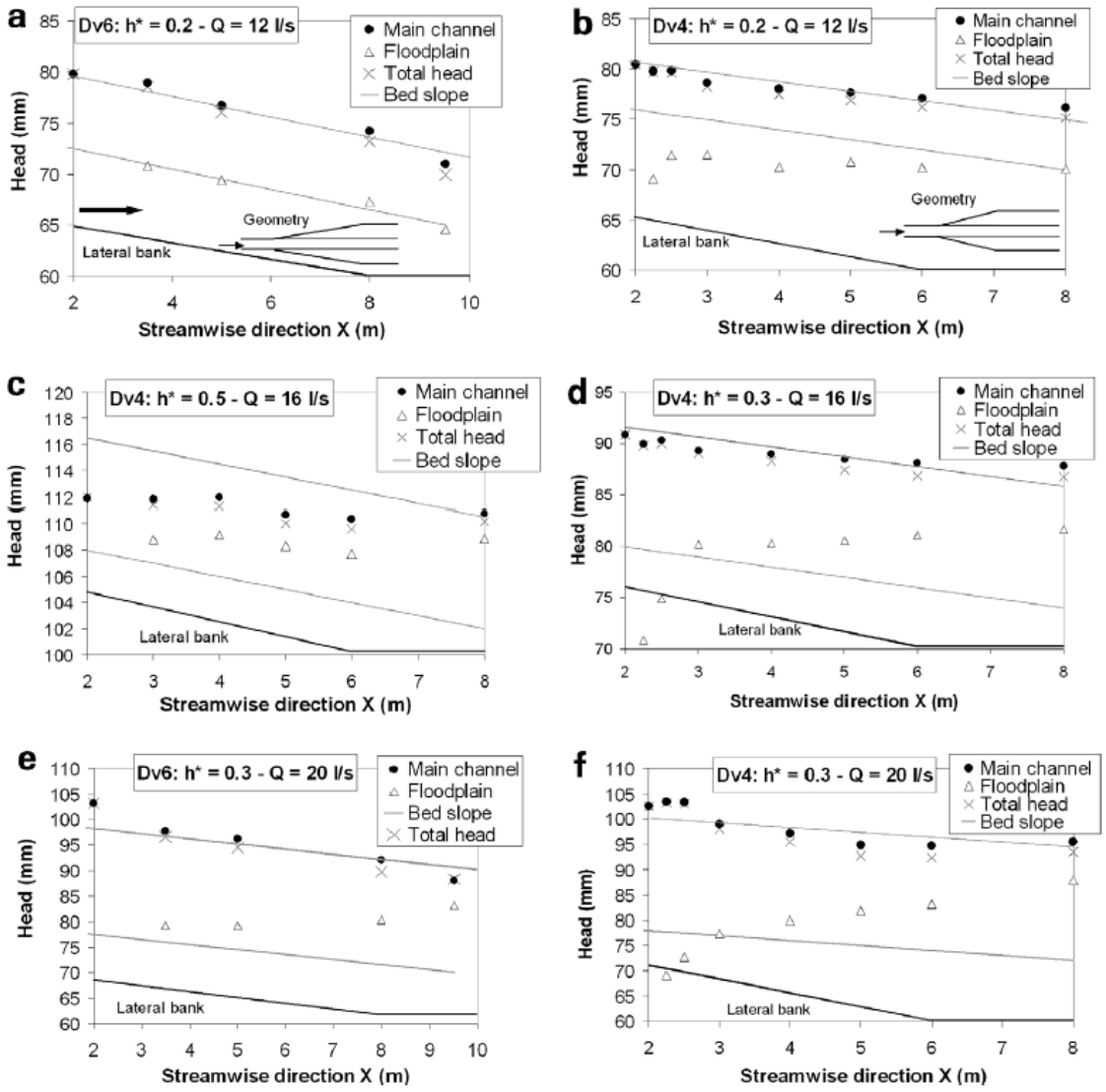

Fig. 6. Experimental sub-section-averaged head (H_i) and total head (H) in diverging geometries Dv4 and Dv6.

Author-produced version of the article published in Advances in Water Resources, 2010, 33 (1), 1-16
The original publication is available at http://www.sciencedirect.com/, doi:10.1016/j.advwatres.2009.10.003

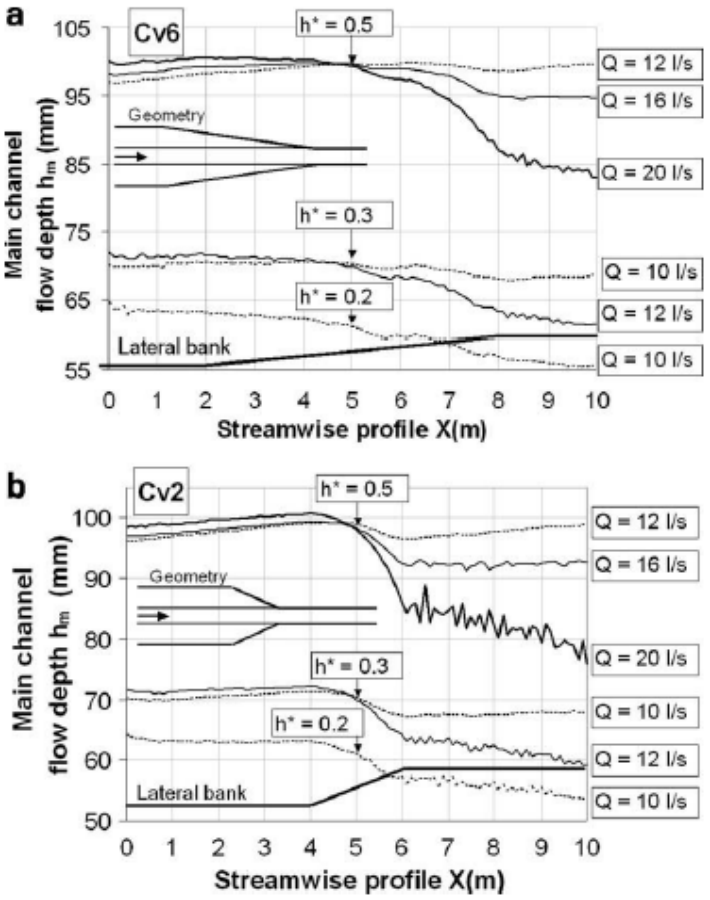

Fig. 7. Longitudinal profile of experimental flow depth in the main channel for converging floodplains Cv6 (a) and Cv2 (b).

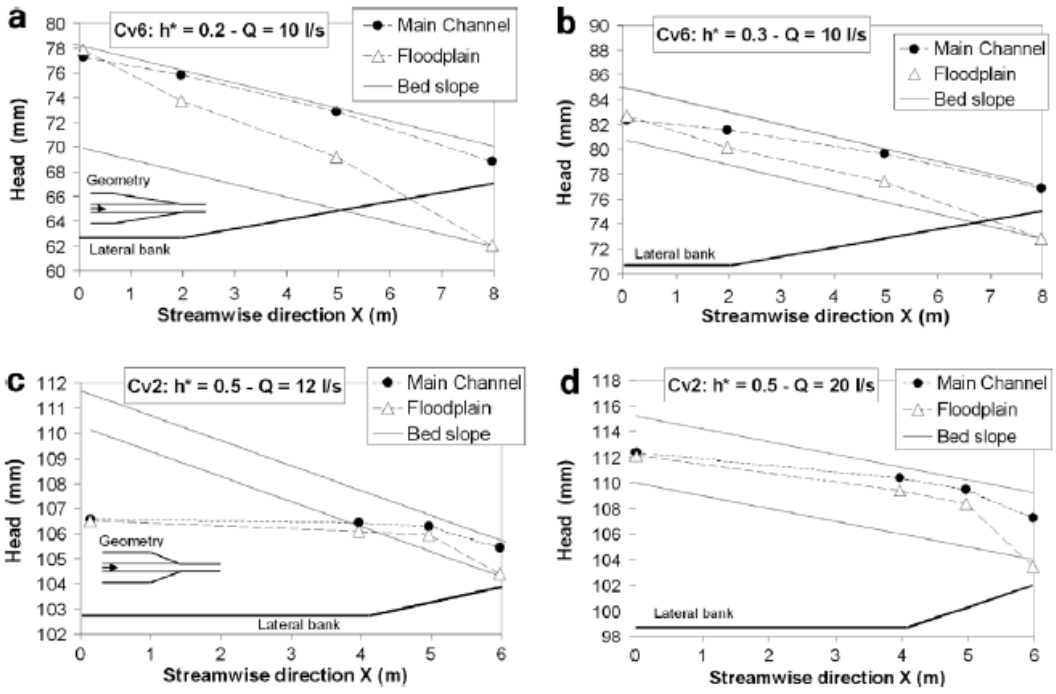

Fig. 8. Experimental sub-section-averaged head H_i in converging geometries Cv2 and Cv6.

Author-produced version of the article published in Advances in Water Resources, 2010, 33 (1), 1-16
The original publication is available at http://www.sciencedirect.com/, doi:10.1016/j.advwatres.2009.10.003

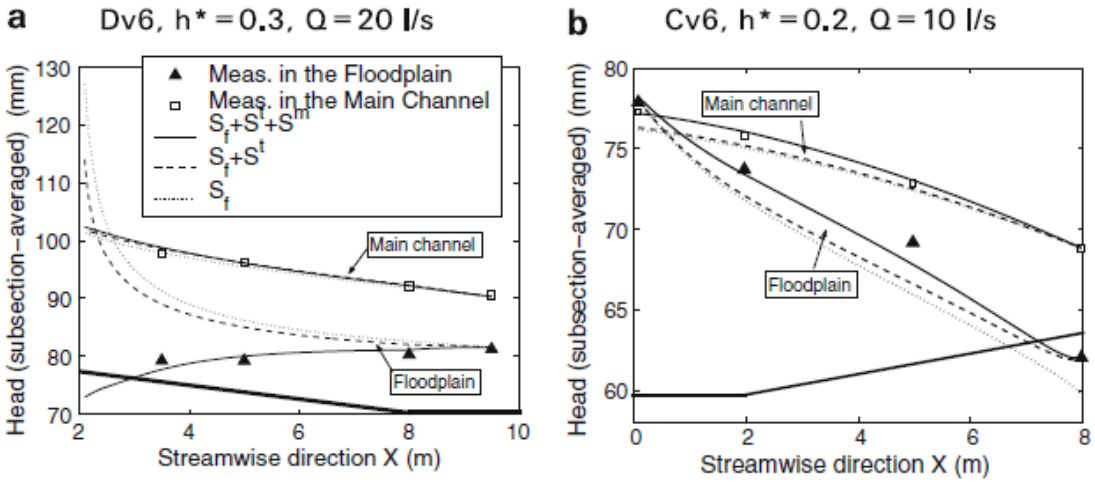

Fig. 9. ISM results versus measurements of sub-section head in converging or diverging geometries (Cv6 and Dv6, $\delta = 3.8°$)

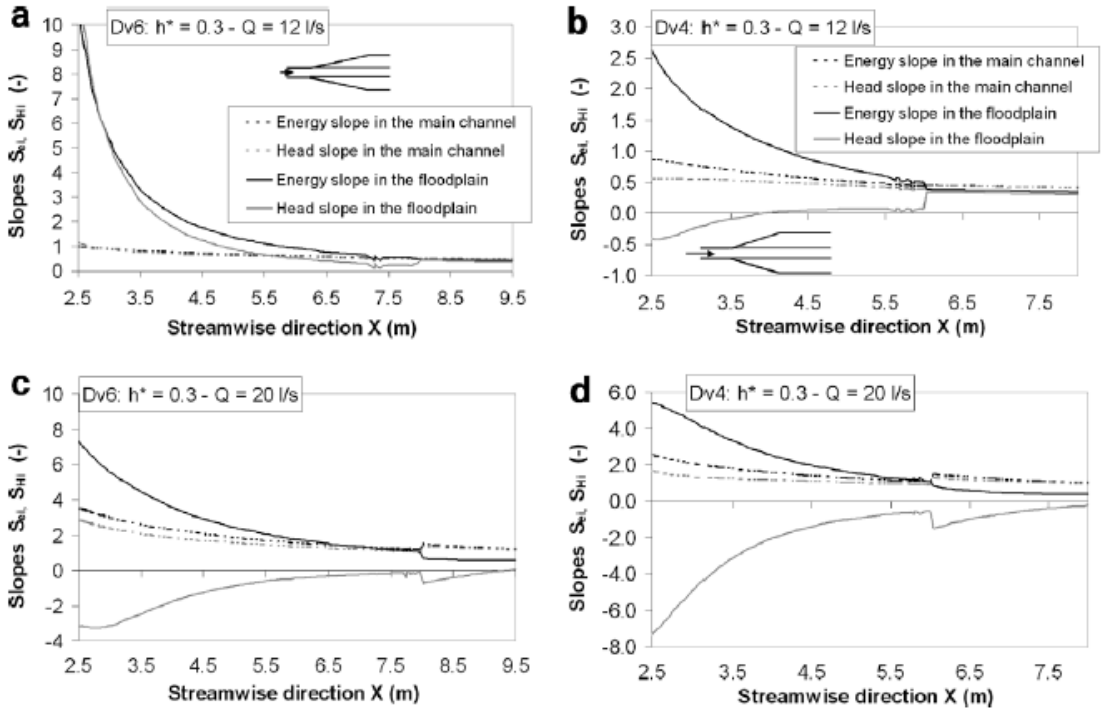

Fig. 10. Head slope gradient S_{Hi} and energy slope S_{ei} in the sub-sections for flows in diverging geometries Dv4 and Dv6.

Author-produced version of the article published in Advances in Water Resources, 2010, 33 (1), 1-16
The original publication is available at http://www.sciencedirect.com/, doi:10.1016/j.advwatres.2009.10.003

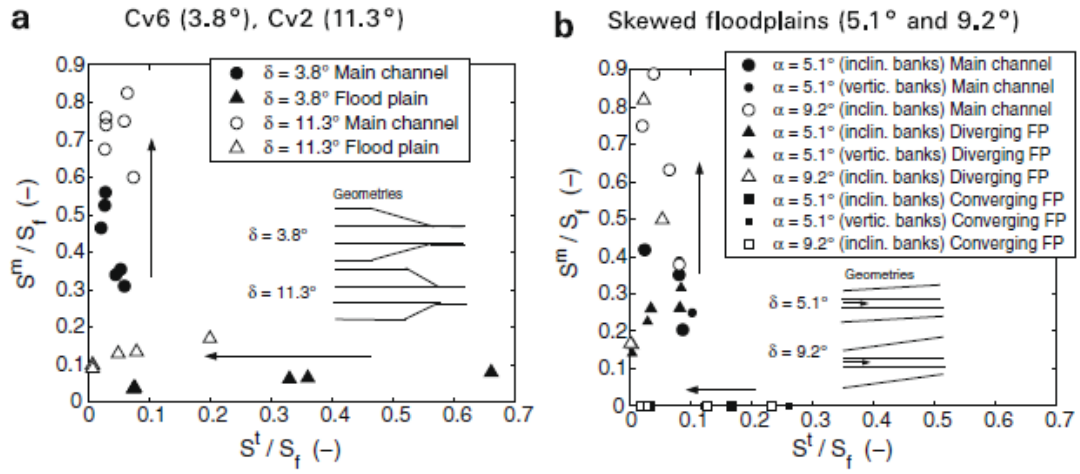

Fig. 11. Effect of the angle δ on head loss due to mass exchange S^m and head loss due to turbulent diffusion S^t: maximum values of S^m / S_f and S^t / S_f ratios in the sub-sections. Arrows indicate the increase in angle δ.

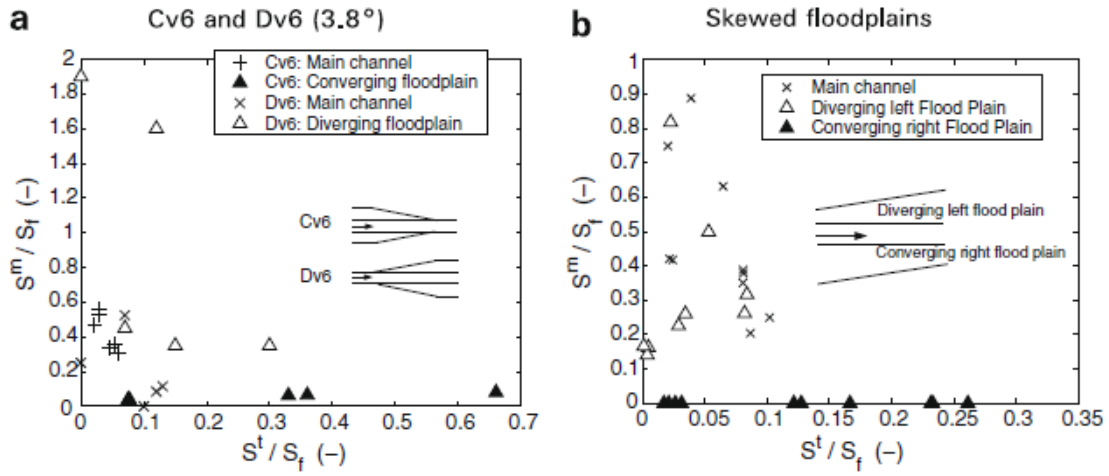

Fig. 12. Converging floodplains vs diverging floodplains for a given δ angle: maximum values of S^m / S_f and S^t / S_f ratios in the sub-sections.

Author-produced version of the article published in Advances in Water Resources, 2010, 33 (1), 1-16
The original publication is available at http://www.sciencedirect.com/, doi:10.1016/j.advwatres.2009.10.003

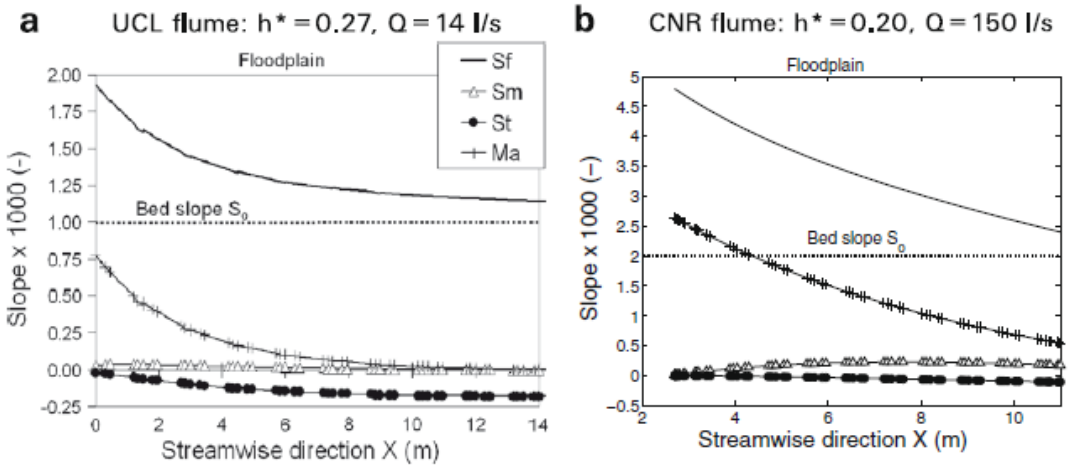

Fig. 13. Developing flow in straight geometries: friction slope S_f, head loss due to mass exchange S^m, head loss due to turbulent diffusion S^t, and mass conservation term Ma as modeled by the ISM (values in the floodplain).

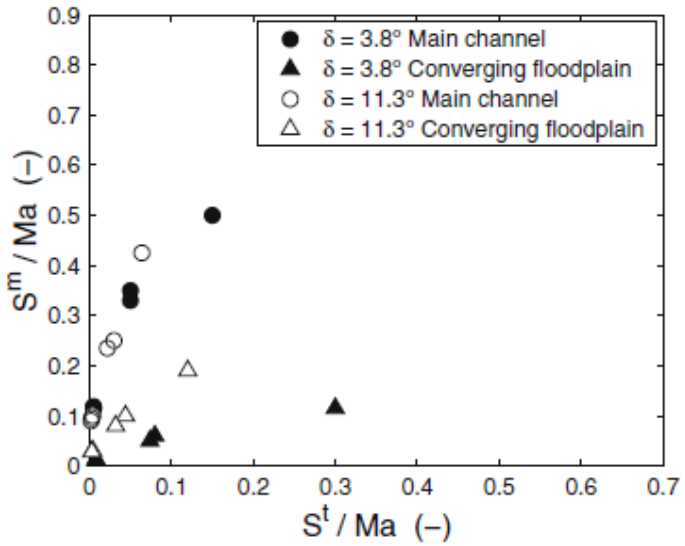

Fig. 14. Flows in converging geometries Cv6 and Cv2: maximum values of S^t / Ma and S^m / Ma ratios in the sub-sections.